Nuclear models in FLUKA: present capabilities, open problems and future improvements

INTERNATIONAL CONFERENCE ON NUCLEAR DATA

FOR SCIENCE & TECHNOLOGY

September 30 2004

Santa Fé

F. Ballarini[4], G. Battistoni[0], F. Cerutti[0], A. Empl[1], A. Fassò[2], A. Ferrari[3], E. Gadioli, M.V. Garzelli[0], A. Ottolenghi[4], L.S. Pinsky[1], J. Ranft[6], S. Roesler[7], P.R. Sala[0], G. Smirnov[8]

[0] University of Milan and INFN, Italy
[1] Houston University, Texas, USA
[2] SLAC, Stanford, USA
[3] CERN (on leave from INFN-Milan)
[4] University of Pavia and INFN, Italy
[5] INFN Frascati, Italy
[6] Siegen University, Germany
[7] CERN
[8] JINR, Dubna, Russia

Topics

- Generalities and general philosophy of FLUKA models
- The FLUKA High energy hadronic models
  - Short description
- The FLUKA Low-intermediate energy hadronic models
  - Short summary and thin target benchmarks
  - “Exotic” applications: neutrino physics
- Examples of complex applications
  - Activation and residual dose rate experiments at CERN
- Nucleus-nucleus interactions in FLUKA
  - Status and (one) example
  - ElectroMagnetic dissociation: an intriguing process

FLUKA: generalities

⋆ Interaction and transport Monte Carlo code

- Hadron-hadron, hadron-nucleus, and γ-nucleus interactions 0-10000 TeV
- Nucleus-nucleus interactions 0-10000 TeV/n
- Electromagnetic and μ interactions 1 keV-10000 TeV
- Neutrino interactions and nucleon decays

⋆ Proven capabilities in:

- Accelerator design and shielding (standard tool at CERN for beam-machine and radioprotection studies)
- ADS studies and experiments
- Dosimetry and hadrotherapy
- Space radiation and cosmic ray showers in the atmosphere (Support by NASA, "de facto" standard tool for all aircraft dosimetry studies in Europe)

Design philosophy: the highest priorities

★ Sound and modern physics

- Based, as far as possible, on original and well tested microscopic models
- All steps (Glauber-Gribov cascade, (G)INC, preequilibrium, evaporation/fragmentation/fission) are self-consistent and have solid physical bases
- Performances optimized by comparing with experimental data at single interaction level: "theory driven, benchmarked with data"
- Final predictions obtained with minimal free parameters fixed for all energies/target/projectiles
- Results in complex cases, as well as properties and scaling laws, arise naturally from the underlying physical models
- Basic conservation laws fulfilled "a priori"

$\Longrightarrow$ Predictivity where no experimental data are directly available

★ Monte Carlo exclusive event generators

- Correlations preserved fully within interactions and among shower components
- Suitable environment for "exotic" extensions (ν's, nucleon decays etc)

Example: Next generation ν experiments

ν experiments with accelerator, atmospheric and reactor ν, aim to high precision studies, like

- θ_{13} driven "subleading" $\nu_\mu \leftrightarrow \nu_e$ oscillation (% effect)
- CP violation

Plot: 20 GeV p on C, $\rightarrow \pi^+ \rightarrow \nu_\mu$ oscillation at 730 km $\rightarrow \nu_e$

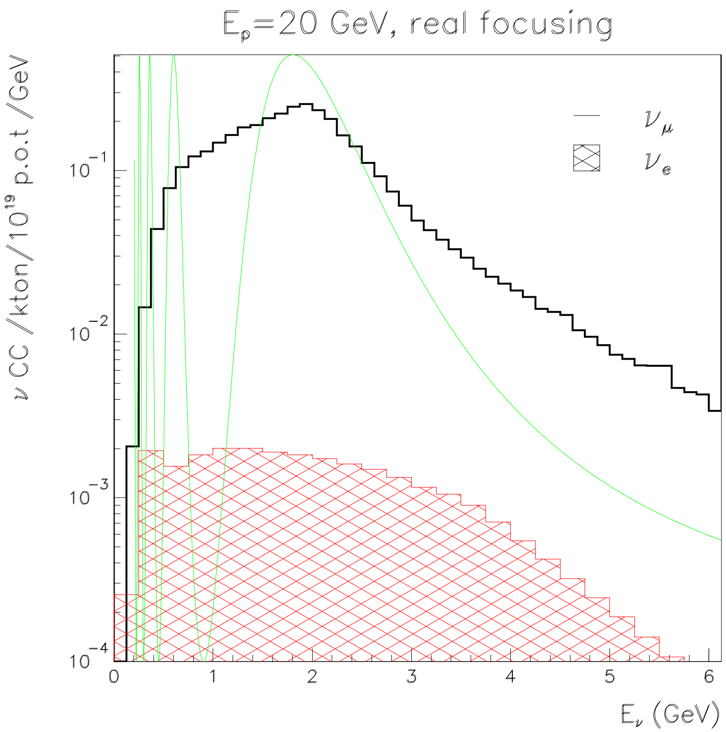

Mandatory: high precision in:

- ν spectra calculation from
  - Cosmic rays showers (from multi-TeV to sub GeV, + heavy ions)
  - "Super-beams" and β-beams from accelerators (few GeV, π production and transport)
- ν interactions down to the sub-GeV range Nuclear effects

Neutrino quasi-elastic events

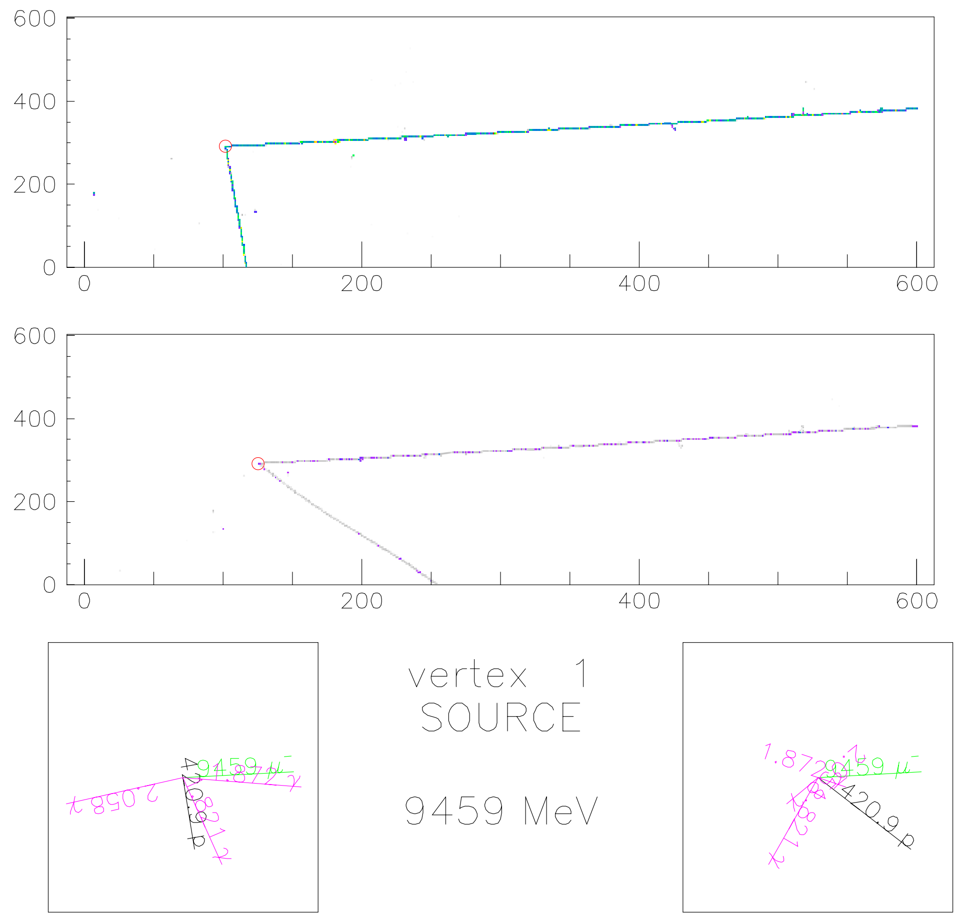

ICARUS prototype: two views in Liquid Argon, 10 GeV ν_μ QE CC

"Clean" event :

$$\nu_\mu \; n \longrightarrow \mu^- \; p$$
$$\downarrow$$
$$\mu^- \;\; \mathrm{p} \; \gamma$$

Neutrino quasi-elastic events

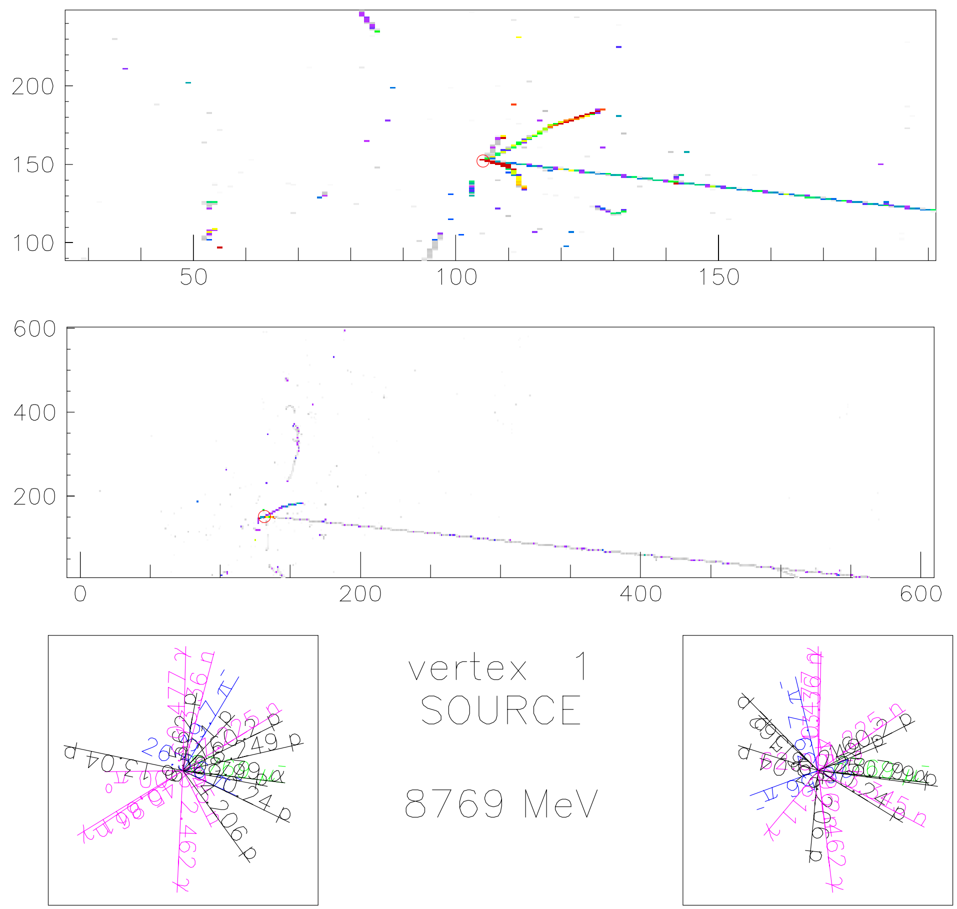

ICARUS prototype: two views in Liquid Argon, 10 GeV ν_μ CC

Complex QE CC event :

$$\nu_\mu\, n \rightarrow \mu^-\, p$$

$$\downarrow$$

1 μ^-, 8 p, 2 π^-, 1 π^0, 4 n, 1 α, 3 γ

The FLUKA hadronic models

Hadron-Nucleon

Elastic, exchange	P<3-5GeV/c	low E π,K	High Energy
Phase shifts, data,eikonal	Resonance prod. and decay	Special	DPM hadronization

Hadron-Nucleus

P<4-5GeV/c	High Energy
PEANUT:	Glauber-Gribov
Sophisticated GINC	multiple interactions
preequilibrium	Coarser GINC
Coalescence	Coalescence

Nucleus-Nucleus

E$>$ 5 GeV/u
DPMJET-III
0.1$<$ E $<$ 5 GeV/u
(modified) rQMD-2.4

Evaporation/Fission/Fermi break-up
γ deexcitation

hA at high energies: Glauber-Gribov cascade with formation zone

★ Dual Parton Model (DPM)

- Interacting strings (quarks held together by the gluon-gluon interaction)
- Each of the two colliding hadrons splits into two colored partons $\longrightarrow$ combination into two color neutral chains $\longrightarrow$ two back-to-back jets
- Each jet is then hadronized into physical hadrons

★ Glauber cascade

- Quantum mechanical method to compute Elastic, Quasi-elastic and Absorption hA cross sections from Free hadron–nucleon scattering + nuclear ground state
- Multiple collision expansion of the scattering amplitude

★ Glauber-Gribov

- Field theory formulation of Glauber model
- Multiple collision terms $\Leftrightarrow$ Feynman graphs
- High energies: exchange of one or more Pomerons (IP) with one or more ($=\nu$) target nucleons (a closed string exchange)

★ Formation zone (= materialization time)

Generalized Intra-Nuclear Cascade: PEANUT

★ Main assets of the full GINC as implemented in FLUKA below 5 GeV:

- PEANUT (PreEquilibrium Approach to NUclear Thermalization): GINC + preequilibrium stage handling nucleons, pions, kaons, γ, stopping μ^- and ν's
- Nucleus divided into 16 radial zones of different density, plus 6 outside the nucleus to account for nuclear potential, plus 10 for charged particles
- Different nuclear densities for neutrons and protons
- Nuclear (complex) optical potential $\Longrightarrow$ curved trajectories in the mean nuclear+Coulomb field (reflection, refraction)
- Updating binding energy (from mass tables) after each particle emission
- Multibody absorption for $\pi^{+/0/-}$, $K^{-/0}$, μ^-
- Energy-momentum conservation including the recoil of the residual nucleus
- Nucleon Fermi motion including wave packet-like uncertainty smearing
- Quantum effects (mostly suppressing): Pauli blocking, Formation zone, Nucleon antisymmetrization, Nucleon-nucleon hard-core correlations, Coherence length

Nuclear effects in ν interactions - I

ν interactions in FLUKA: ν-nucleon int. integrated in PEANUT nuclear environment. Quasi-elastic built-in, Resonant and deep-inelastic presently from NUX generator (NUX-FLUKA in Proceedings of NUINT04, in press).

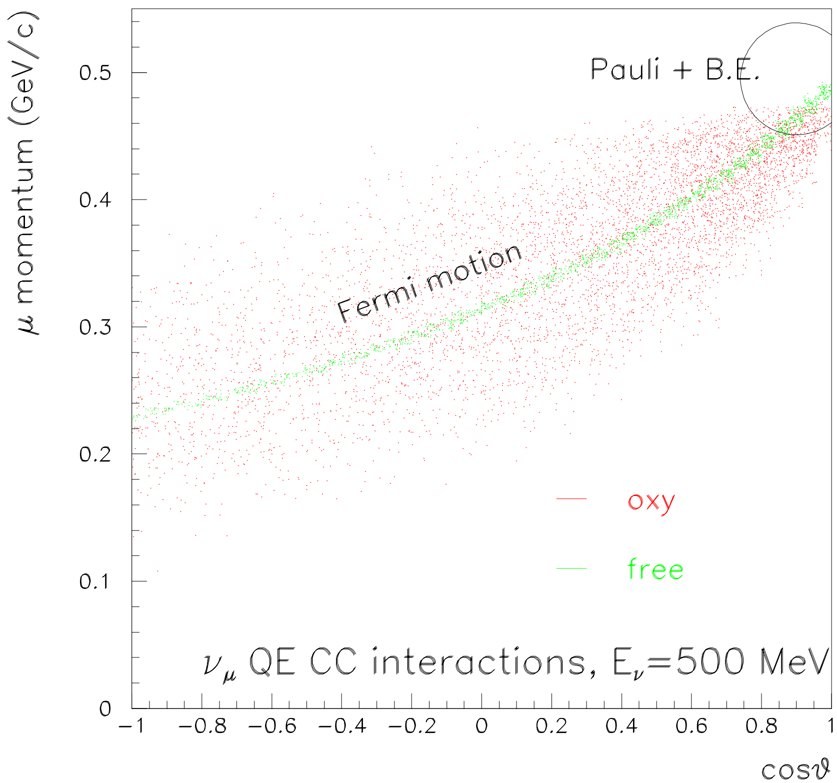

Angle-Momentum correlation of the outgoing μ in Quasi Elastic ν_μ interactions, on free neutrons and on Oxygen nuclei. Initial State effects are evident.

Formation zone

Naively: "materialization" time. Qualitative estimate: in the frame where $p_{\parallel} = 0$

$$\bar{t} \ = \ \Delta t \approx \frac{\hbar}{E_T} = \frac{\hbar}{\sqrt{p_T^2 + M^2}}$$

particle proper time

$$\tau \ = \ \frac{M}{E_T}\bar{t} = \frac{\hbar M}{p_T^2 + M^2}$$

Going to lab system

$$t_{lab} \ = \ \frac{E_{lab}}{E_T}\bar{t} = \frac{E_{lab}}{M}\tau = \frac{\hbar E_{lab}}{p_T^2 + M^2}$$

Condition for possible reinteraction inside a nucleus:

$$v \cdot t_{lab} \leq R_A \approx r_0 A^{\frac{1}{3}}$$

Coherence length $\equiv$ *formation time for elastic or quasielastic hN interactions (not discussed here)*

Effect of different formation time (τ) values on the total hadron multiplicity and on hadron spectra in ν_μ CC interactions.

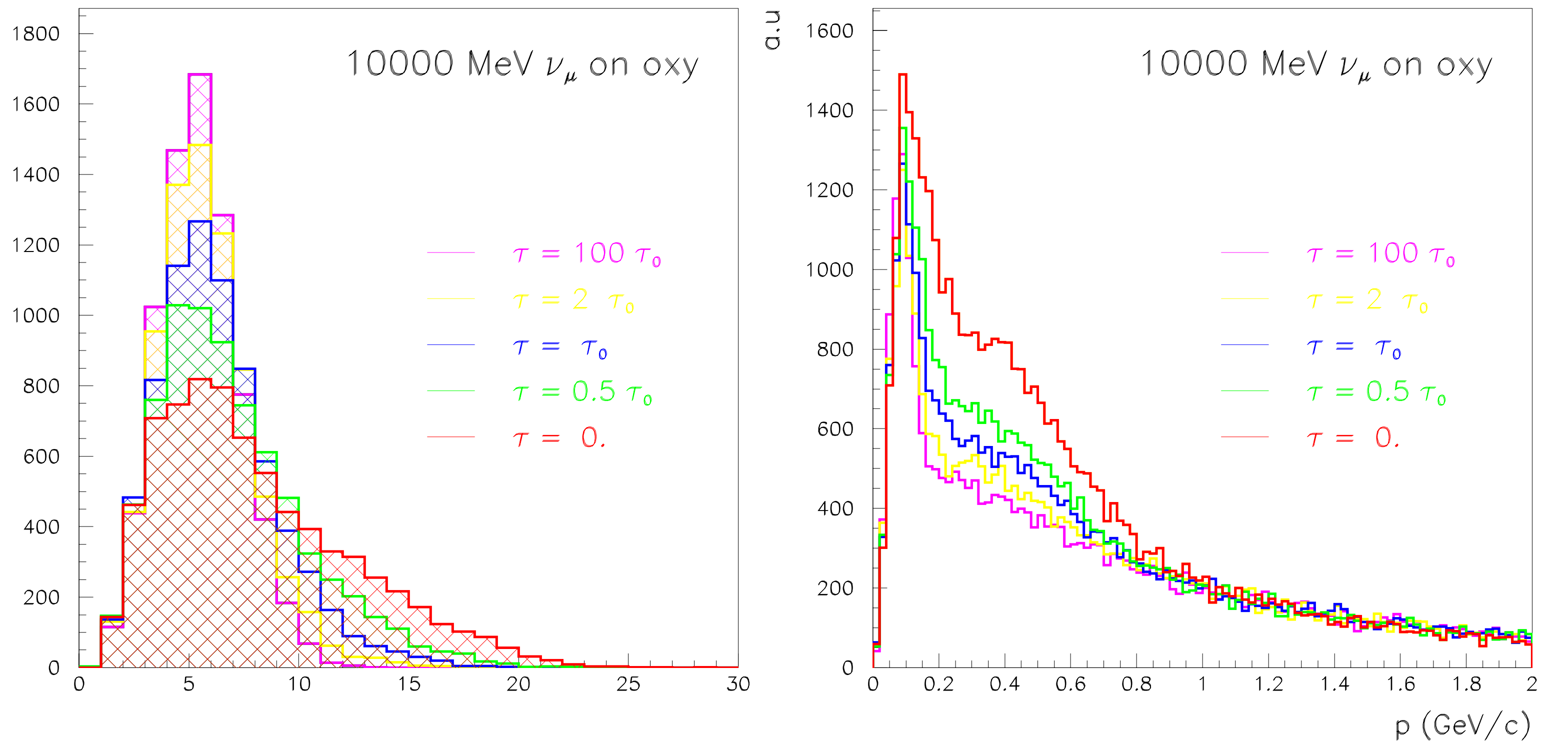

Pions: nuclear medium effects

Pion-nucleon interactions: non-resonant + p-wave resonant Δ's.

Δ in nuclear medium

decay

elastic scattering or charge exchange

reinteraction

pion absorption

$\longrightarrow$ Δ width different from the free one

Assuming a Breit-Wigner for the free resonant cross section with width Γ_F

$$\sigma_{res}^{Free} = \frac{8\pi}{p_{cm}^2} \frac{M_\Delta^2 \Gamma_F(p_{cm})^2}{\left(s - M_\Delta^2\right)^2 + M_\Delta^2 \Gamma_F(p_{cm})^2}$$

Add "in medium" width (Oset et.al ,NPA 468, 631)

$$\frac{1}{2}\Gamma_T = \frac{1}{2}\Gamma_F - \mathrm{Im}\Sigma_\Delta, \quad \Sigma_\Delta = \Sigma_{qe} + \Sigma_2 + \Sigma_3$$

(Σ_{qe}, Σ_2, Σ_3 = widths for quasielastic scattering, two and three body absorption)

Add two-body s-wave absorption cross section from optical model

Nuclear potential for π: Energy dependent, resonant shape (+ Coulomb)

Pions in ν interactions

Charged pion spectra after ν_μ interaction.

Initial State == particles still inside the nucleus

Final State == particles outside the nucleus

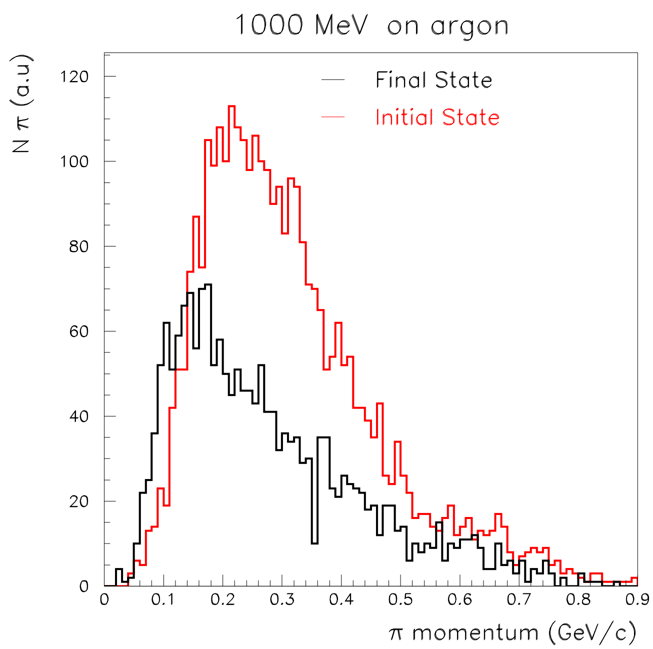

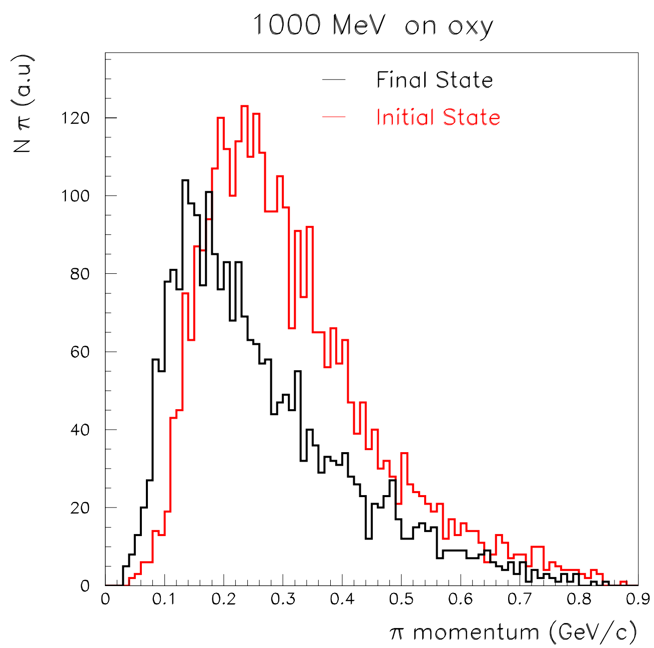

58% escape at 1 GeV on Ar, 75% on Oxygen

Missing Transverse Momentum

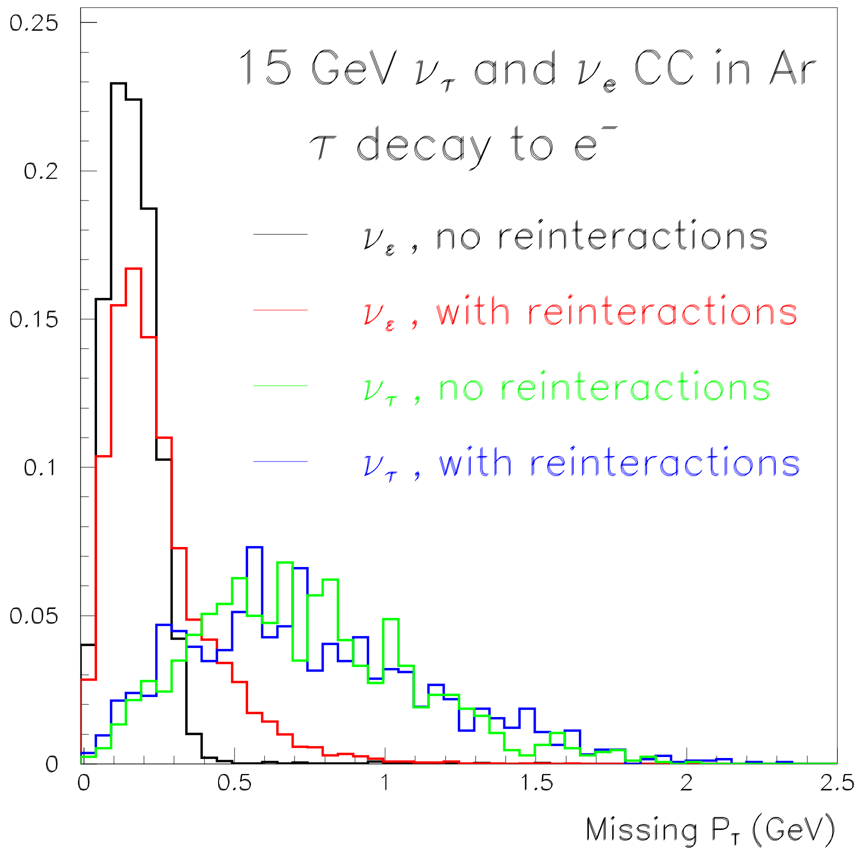

ν_τ identification vs ν_e

(i.e. CNGS ν beam)

One of the possible "cuts" :

missing P_T

$$\nu_\tau + A \rightarrow \tau^- + X \rightarrow e^- + \bar{\nu}_e + \nu_\tau + X$$

Intrinsic Missing P_T due to τ decay

$$\nu_e + A \rightarrow e^- + X$$

No Missing P_T *on free nucleon*

Deeply changed by nuclear effects

Pion production: a key feature for future accelerator projects

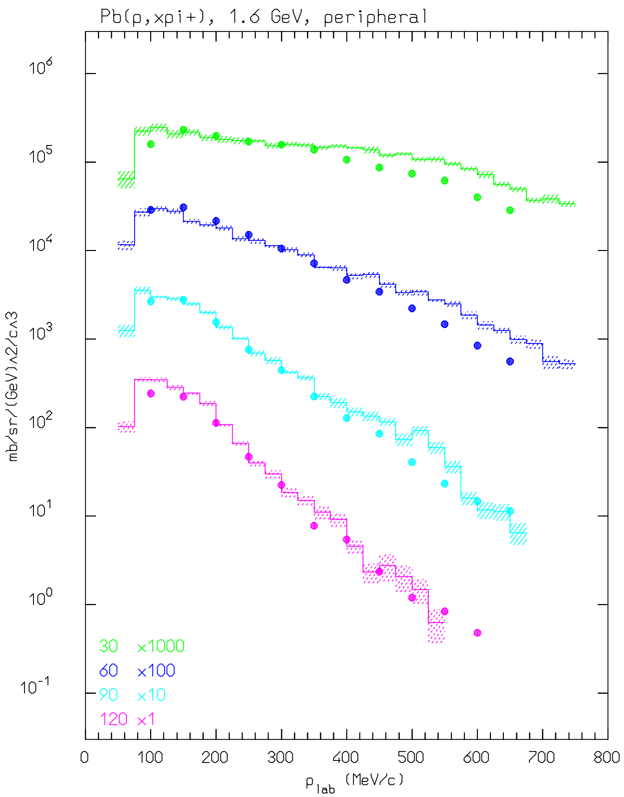

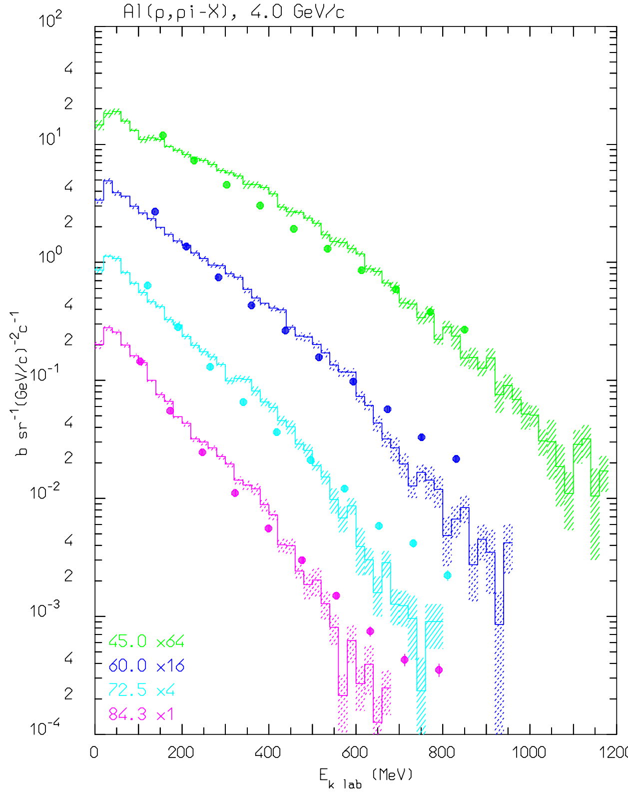

Double differential distributions of π^+'s produced by 1.6 GeV protons on Pb (left), and π^- produced by 4 GeV/c protons on Al (right). Histograms: computed with FLUKA;
symbols: experimental data from: M.C.Lemaire et. al., Report CEA-N-2670, H. En'yo et al, PL 159B, (1985) 1

Preequilibrium in FLUKA

FLUKA preequilibrium is based on GDH (*M. Blann et al.*) cast in a MonteCarlo form

GDH: Exciton model, ρ,E_F are "local" averages on the trajectory and constrained state densities are used for the lowest lying configurations.

Modifications of GDH in FLUKA:

- σ_{inv} from systematics
- Correlation/coherence length/ hardcore effect on reinteractions
- Constrained exciton state densities configurations 1p-1h, 2p-1h, 1p-2h, 2p-2h, 3p-1h and 3p-2h
- True local ρ,E_F for the initial configuration, evolving into average
- Non-isotropic angular distribution (fast particle approximation)

Preequilibrium/(G)INC transition

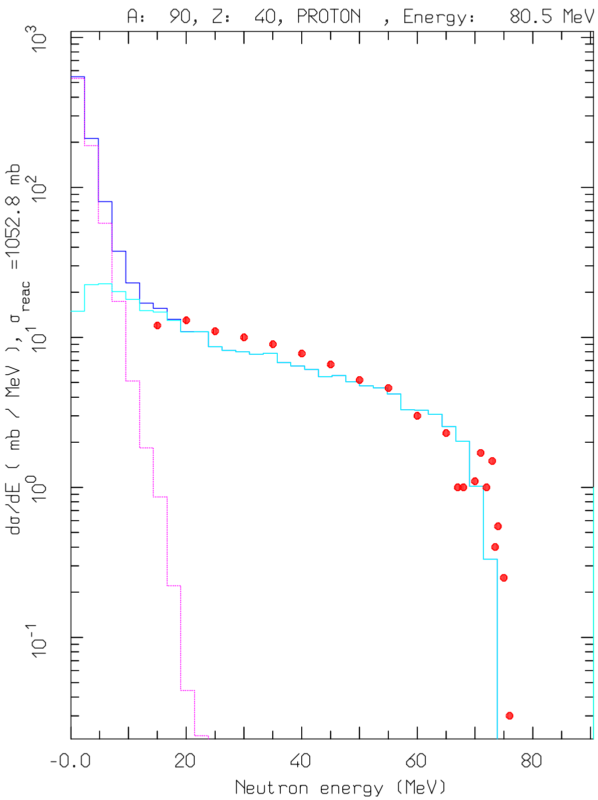

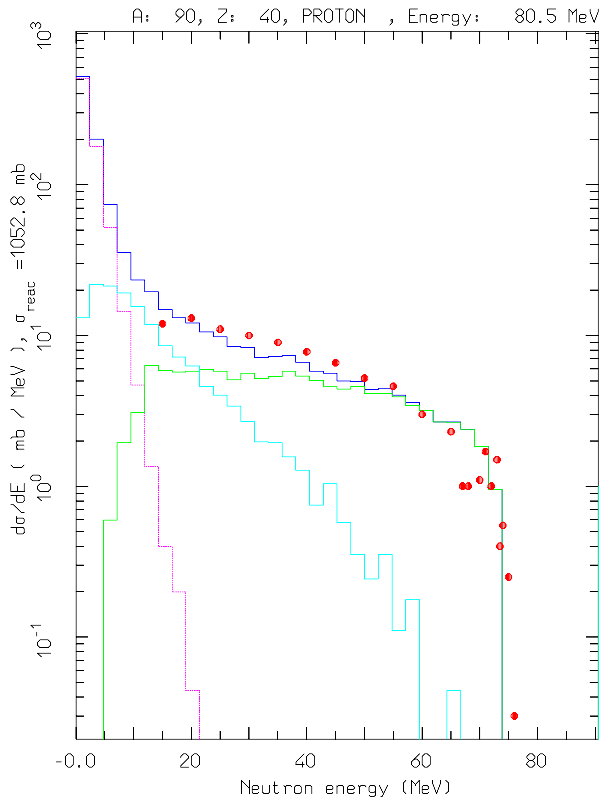

Example of angle integrated ^{90}Zr(p,xn) at 80.5 MeV calculations with the full algorithm (right), and without the INC stage (left). The various lines show the total, INC, preeq. and evaporation contributions, the exp. data have been taken from M.Trabandt et al. **PRC39** (1989) 452

Nucleon emission: thin target examples

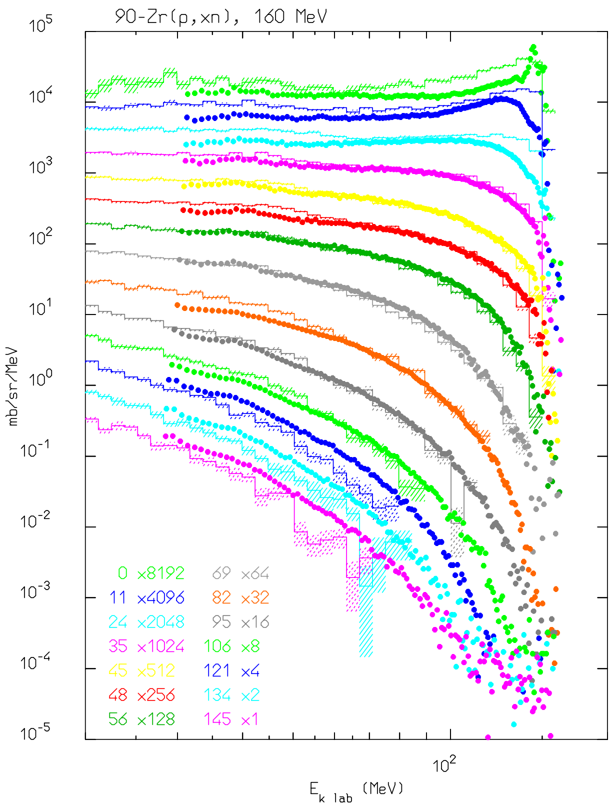

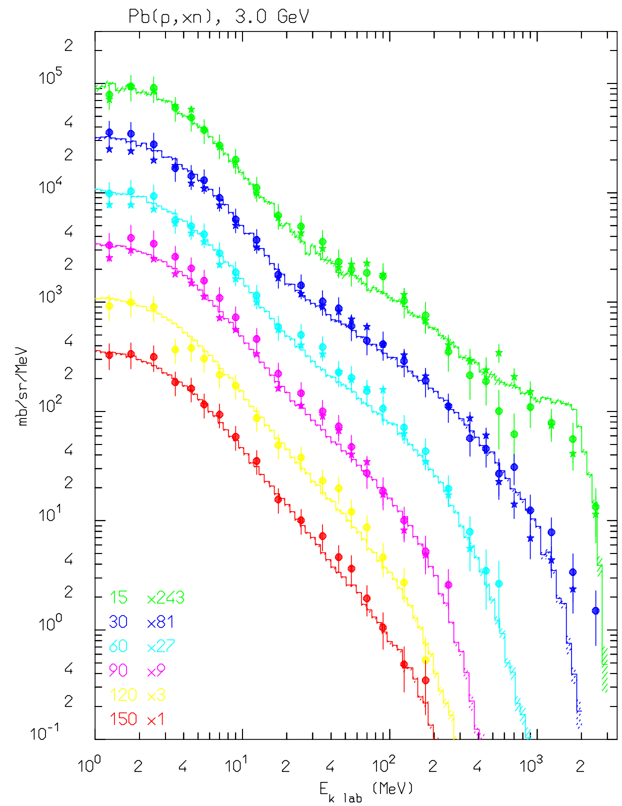

Double differential neutron distributions for Zr(p,xn) at 160 MeV (left) and Pb(p,xn) at 3 GeV (right)

Histograms: computed with FLUKA; symbols: experimental data from

Scobel et al., Phys. Rev. **C41** (1990), 2010, and Ishibashi et al., Nucl. Sci. Technol. **32** (1995) 827

PEANUT: example of coalescence

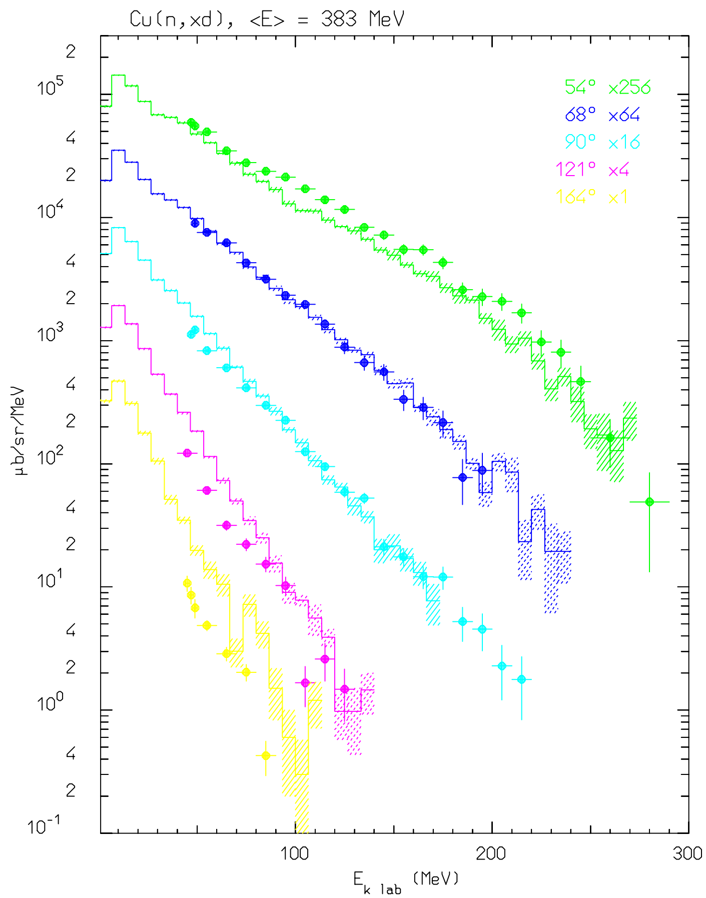

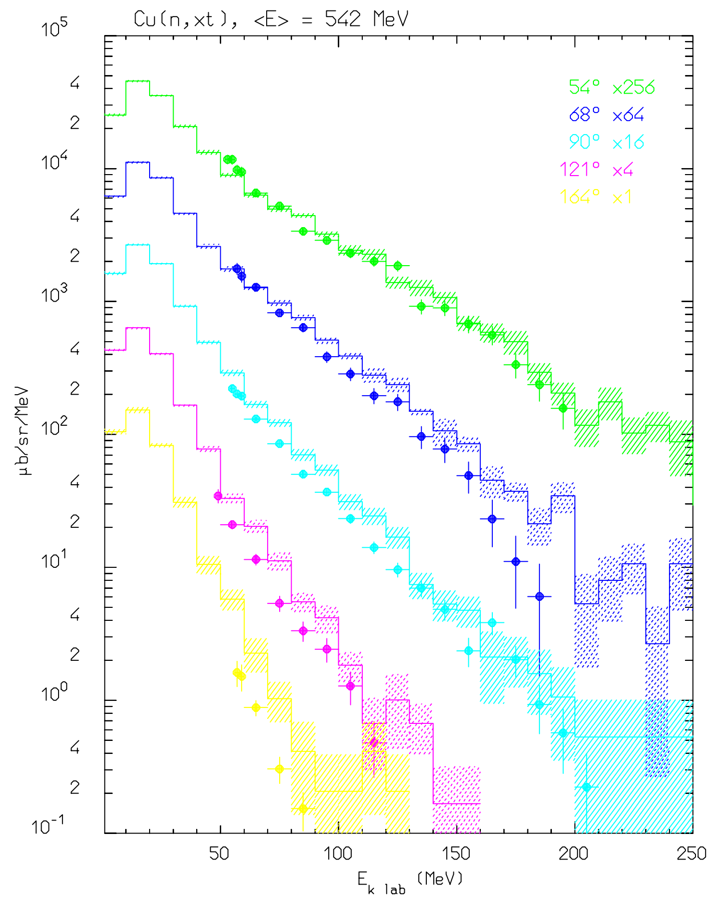

Deuteron (left) and triton (right) emission from 383 and 542 MeV neutrons on Cu.

Data (symbols): J. Franz et al.,Nucl. Phys. **A510**, 774 (1990)

Equilibrium particle emission

⋆ Evaporation: Weisskopf-Ewing approach

- $\boxed{\text{New!!}}$ $\approx$ 600 possible emitted particles/states (A$\leq$24) with an extended evaporation/fragmentation formalism
- Full level density formula with level density parameter A,Z and excitation dependent
- Inverse cross-sections with proper sub-barrier
- Analytic solution for the emission widths (neglecting the level density dependence on U, taken into account by rejection)
- Emission energies from the width expression with no approx.

⋆ Fission: improved version of the Atchison algorithm

- Improved mass and charge widths
- Full competition with evaporation

⋆ Fermi Break-up for A$\leq$17 nuclei

- $\approx$ 50,000 combinations included with up to 6 ejectiles

⋆ γ de-excitation: statistical + rotational + tabulated levels

Residual nuclei: the mass distribution at high energies

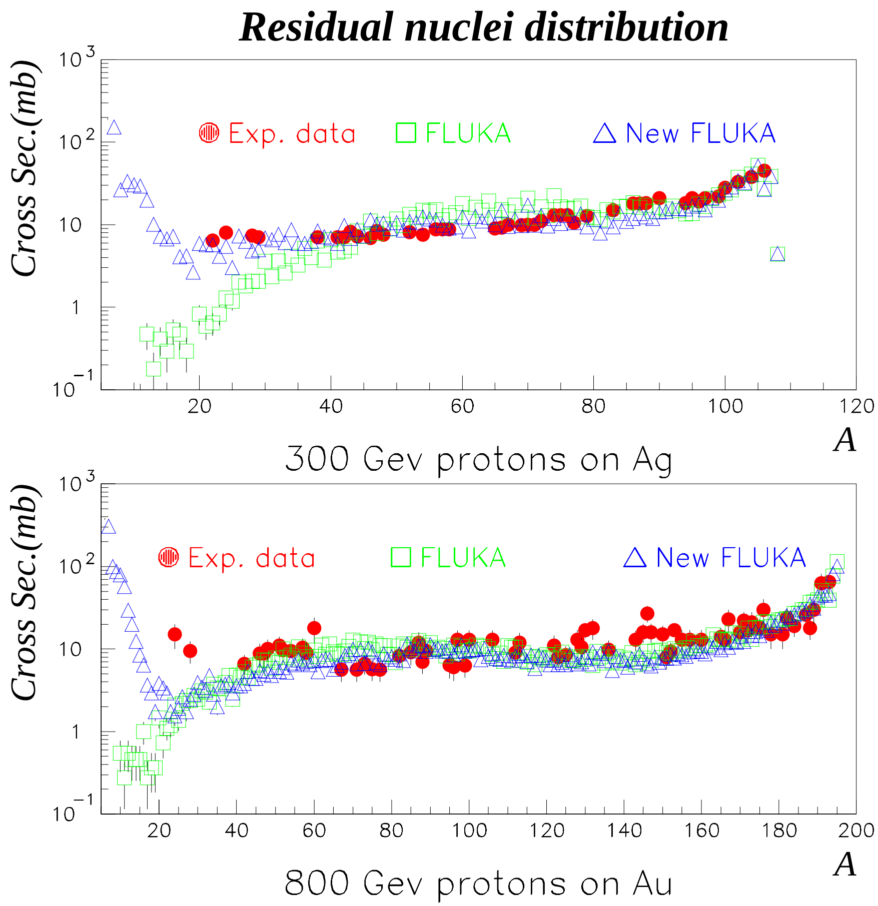

Experimental and computed residual nuclei mass distribution for Ag(p,x)X at 300 GeV (top) and Au(p,x)X at 800 GeV (bottom) (data from PRC19 2288 (1979) for silver, and NPA543 703 (1992) for gold).

CERN activation and dose rate benchmark

Irradiated samples at the CERF facility (CERN) (M.Brugger et al., Proc. ICRS10, in press)

120 GeV mixed p, π^+, K^+ beam on a thick Cu target

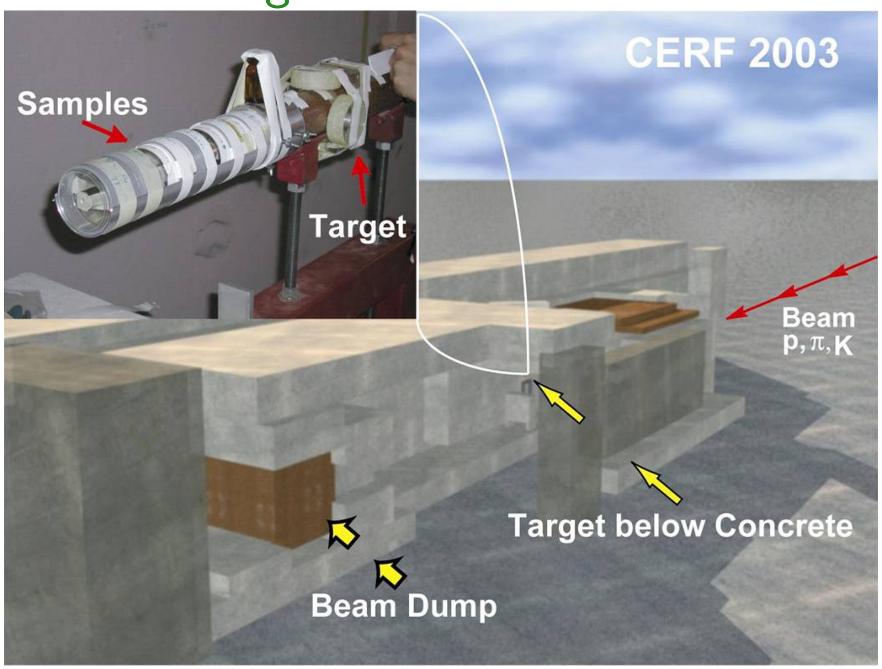

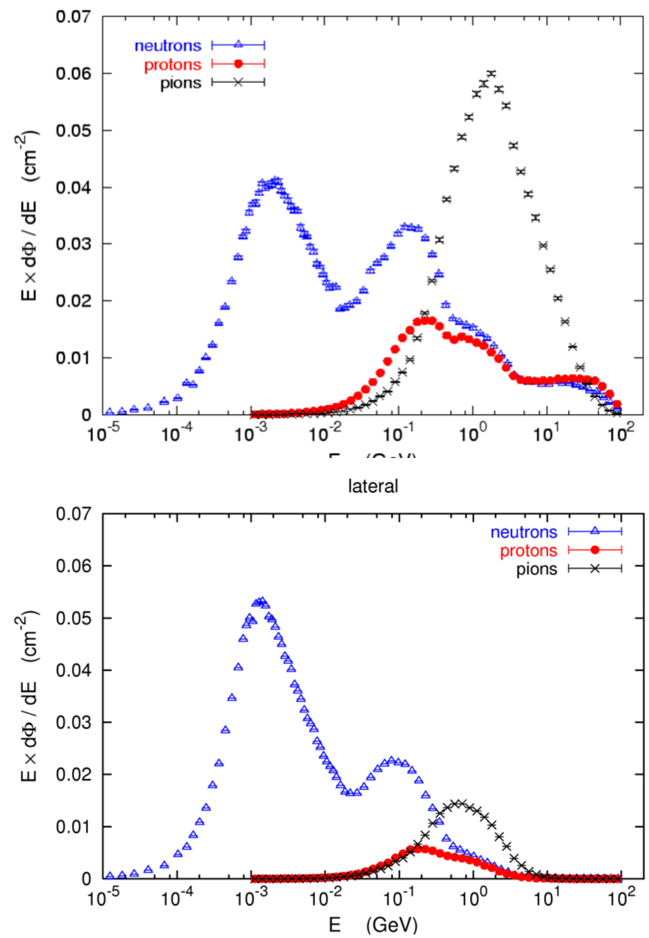

CERN activation benchmark: Stainless Steel

Table 1: Stainless Steel, cooling times 1d 6h 28m, 17d 10h 39m

Isotope	$t_{1/2}$	Exp Bq/g	± %	STD FLUKA/Exp	± %	NEW FLUKA/Exp	± %
Be 7	53.29d	0.205	24	0.096	34	1.070	30
Na 24	14.96h	0.513	4.3	0.278	8.6	0.406	13
K 43	22.30h	1.08	4.6	0.628	8.7	0.814	11
Ca 47	4.54d	0.098	25	0.424	44	(0.295	62)
Sc 44	3.93h	13.8	4.8	0.692	5.8	0.622	6.2
mSc 44	58.60h	6.51	7.1	1.372	8.1	1.233	8.6
Sc 46	83.79d	0.873	8.3	0.841	9.1	0.859	9.5
Sc 47	80.28h	6.57	8.2	0.970	9.7	1.050	13
Sc 48	43.67h	1.57	5.2	1.266	8.4	1.403	11
V 48	15.97d	8.97	3.1	1.464	3.8	1.354	4.8
Cr 48	21.56h	0.584	6.7	1.084	11	1.032	12
Cr 51	27.70d	15.1	12	1.261	13	1.231	13
Mn 54	312.12d	2.85	10	1.061	10	1.060	11
Co 55	17.53h	1.04	4.6	1.112	7.7	0.980	10
Co 56	77.27d	0.485	7.6	1.422	9.0	1.332	10
Co 57	271.79d	0.463	11	1.180	12	1.140	12
Co 58	70.82d	2.21	5.9	0.930	6.3	0.881	6.9
Ni 57	35.60h	3.52	4.5	1.477	6.5	1.412	8.2

CERN benchmark: residual dose rates

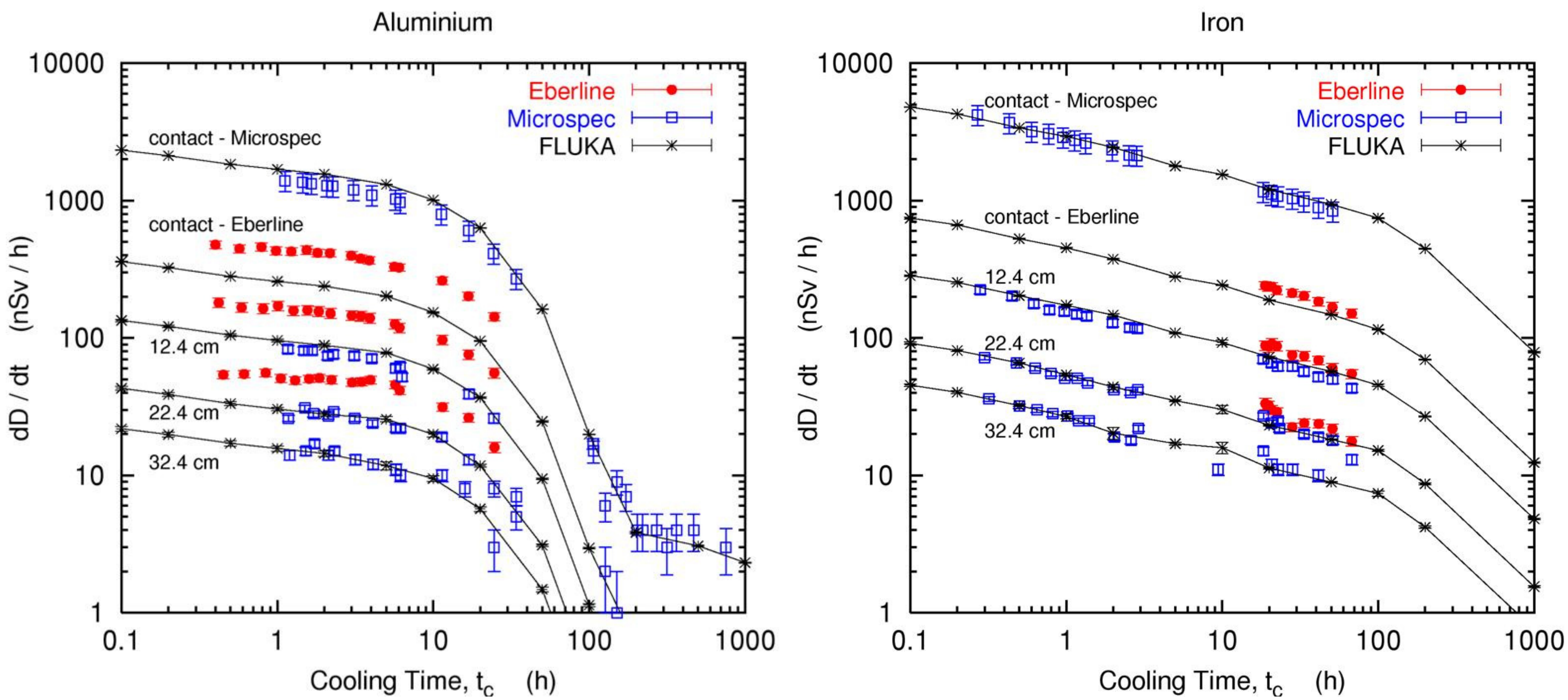

Measured (blue and red symbols, two different instruments), and simulated residual dose rates as a function of time (see M. Brugger et al, Proc. ICRS10 in press, for a thorough discussion of the exp. and simulation methodology).
Left: Aluminium target — Right: Iron target

Nucleon Nucleon interactions: nuclear medium effects

The free NN scattering amplitudes and cross sections must be properly modified for medium effects (Pauli blocking, coherence effects, etc.). The resulting in medium cross sections are density-dependent and smaller than σ_{NNfree}

There are several approaches:

- G.Q.Li et al., PRC48, 1702 (1993); PRC49, 566 (1994) (theoretical, ρ, E and θ dependent)
- C.Xiangzhou et al., PRC58, 572 (1998) (phenomenological, ρ and E dependent)
- R.K.Tripathi et al., NIMB152, 425 (1999); NIMB173, 391 (2001) (phenomenological, only E dependent)
- ...

One of open questions in microscopic models is the (proper) implementation of medium corrected nucleon cross sections. Double counting with explicit Pauli blocking (which is required to get physical events) is an issue, as well as proper correlations with the angular distribution

In-Medium cross sections: example

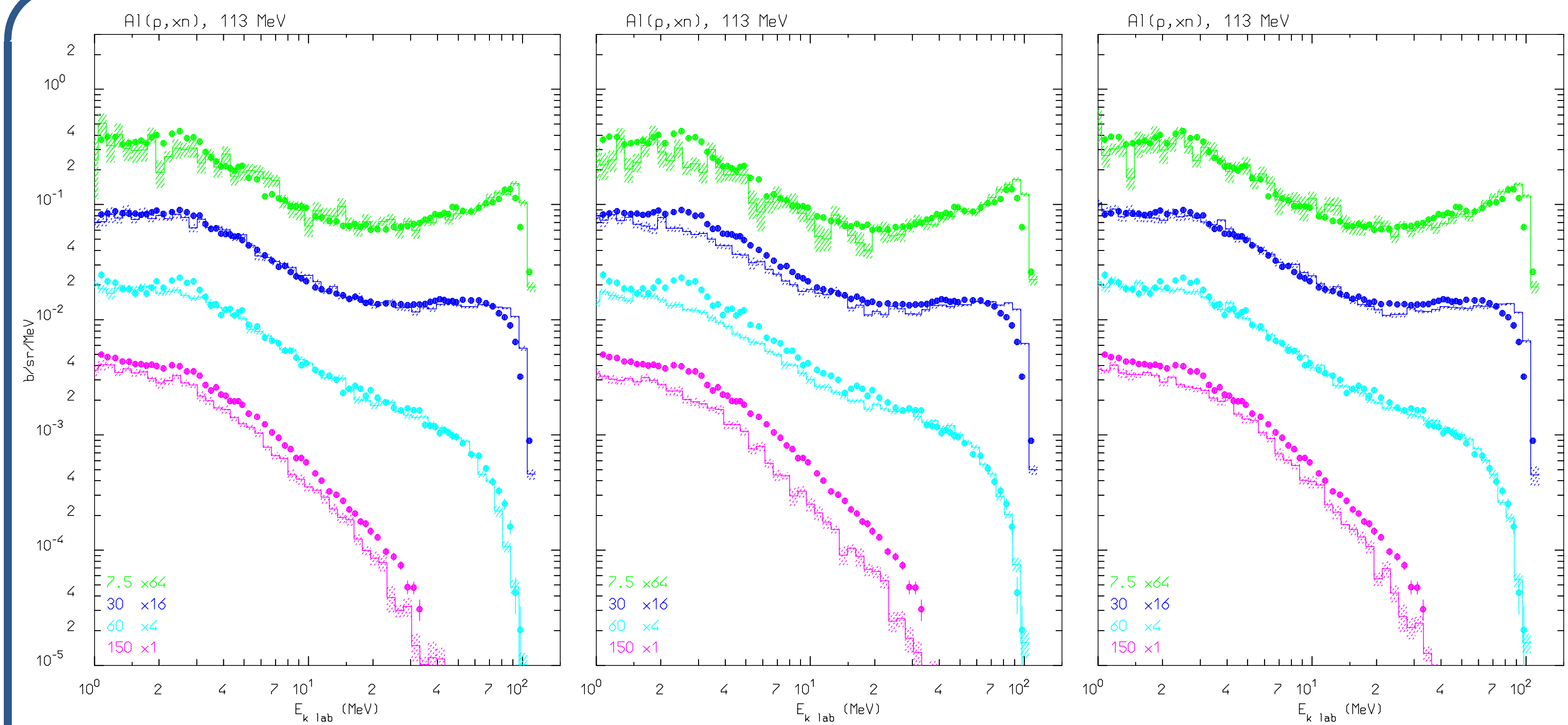

Double differential neutron distributions for Al(p,xn) at 113 MeV. "Normal" PEANUT (left), PEANUT with (Li) in-medium cross sections (center), PEANUT with in-medium cross sections and coherence length, correlation length, and nucleon hard core effects switched off (right). Histograms: computed with FLUKA; symbols: experimental data from Meier et al, Nucl. Sci. Eng. **102** (1989), 310

Heavy ion Interactions models in FLUKA

⋆ DPMJET-III model for energies $\geq$ 5 GeV/n

- DPMJET[1] (R. Engel, J. Ranft, and S. Roesler): Nucleus-Nucleus interaction model
- Energy range: from ≈5-10 GeV/n up to the highest CR energies ($10^{18}-10^{20}$ eV)
- Used in many CR shower codes
- Based on the Dual Parton Model and the Glauber model, like the high energy FLUKA hadron-nucleus generator

⋆ Extensively modified and improved version of rQMD-2.4 for 0.1 $<$ E $<$ 5 GeV/n

- rQMD-2.4[2] (H. Sorge et al.): Cascade - Relativistic QMD model
- Energy range: from ≈ 0.1 GeV/n up to several hundreds of GeV/n
- Successfully applied to relativistic A-A particle production over a wide energy range

⋆ Standard FLUKA evaporation/fission/fragmentation used in both cases for Target/Projectile final deexcitation

[1] PRD 51 (1995) 64; Gran Sasso INFN/AE-97/45 (1997); hep-ph/9911232; hep-ph/9911213; hep-ph/0002137, "The Monte Carlo Event Generator DPMJET-III" Proc. MC2000, Springer-Verlag Berlin, Heidelberg, pp. 1033-1038

[2] H. Sorge PRC52 3291 (1995), H.Sorge, H.Stocker, W.Greiner, Ann. Phys. 192 266 (1989), NPA498 567c (1989)

FLUKA with modified RQMD-2.4 (cascade mode) - results

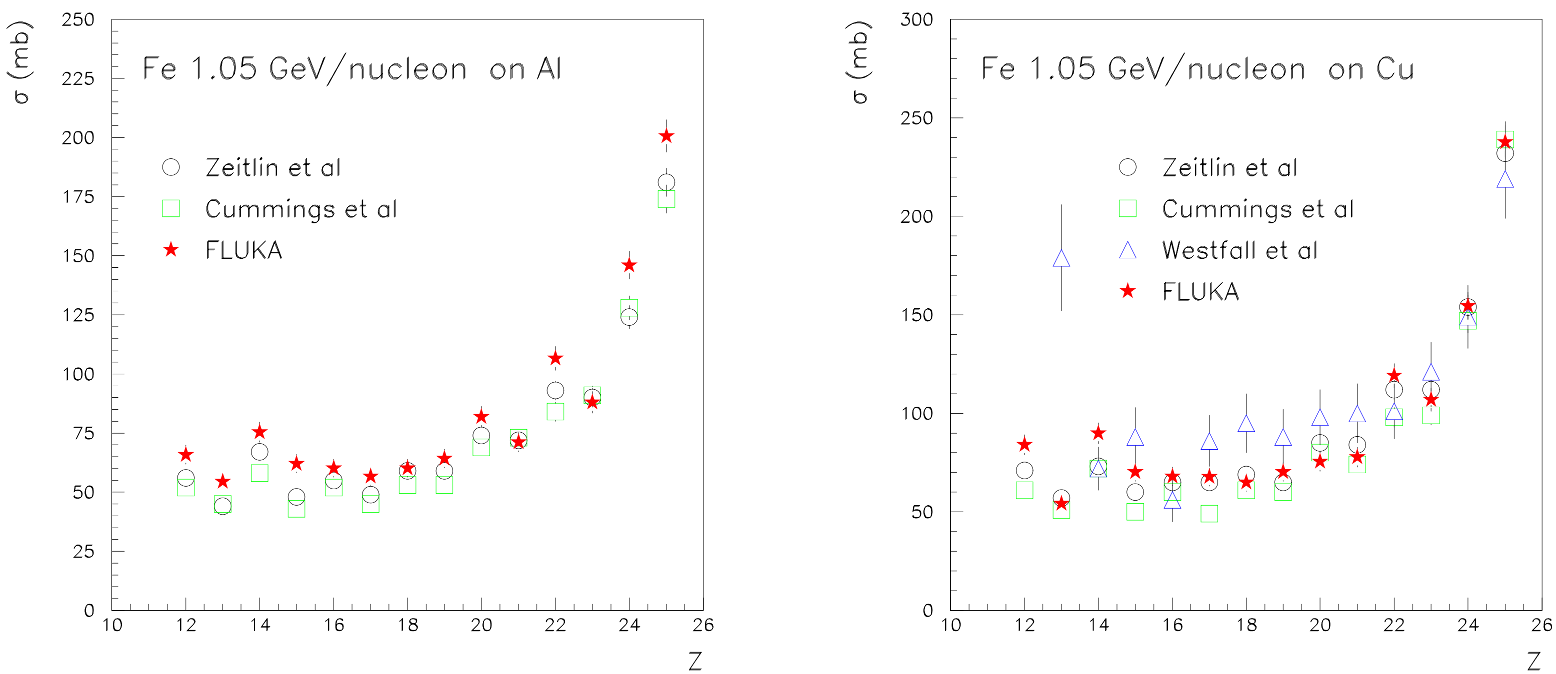

Fragment charge cross sections for 1.05 GeV/n Fe ions on Al (left) and Cu (right). stars FLUKA, circles PRC56 (1997) 388, squares PRC42 (1990) 5208 (at 1.5 GeV/n), triangles PRC19 (1979) 1309 (at 1.88 GeV/n).

Electromagnetic Dissociation

Electromagnetic dissociation: σ_{EM} increasingly large with (target) Z's and energy.
Already relevant for few GeV/n ions on heavy targets ($\sigma_{EM} \approx 1$ b vs $\sigma_{nucl} \approx 5$ b for 1 GeV/n Fe on Pb)

$$\sigma_{1\gamma} = \int \frac{\mathrm{d}\omega}{\omega} n_{A_1}(\omega)\sigma_{\gamma A_2}(\omega), \quad n_{A_1}(\omega) \propto Z_1^2$$

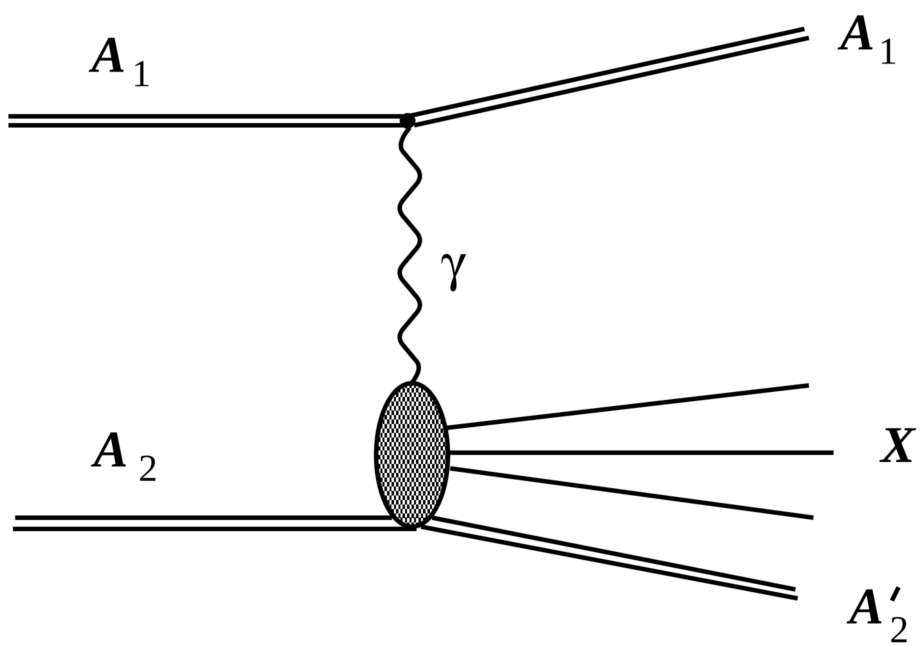

Electromagnetic dissociation: example

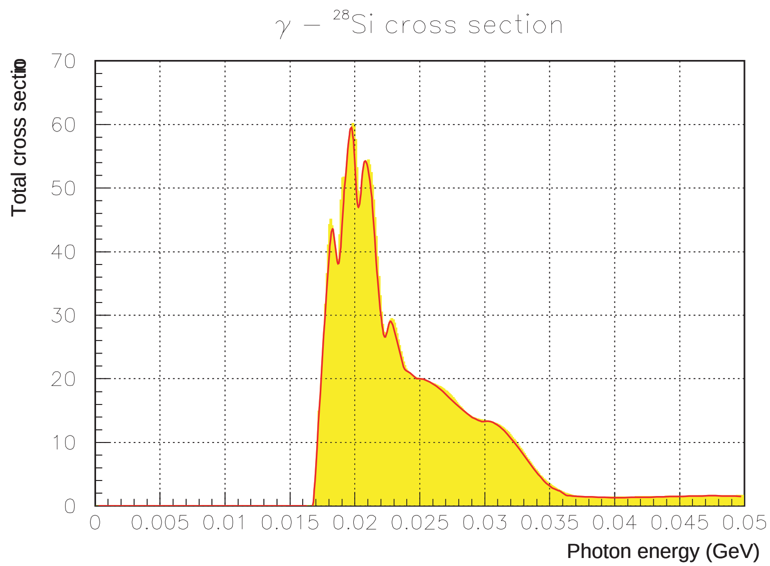

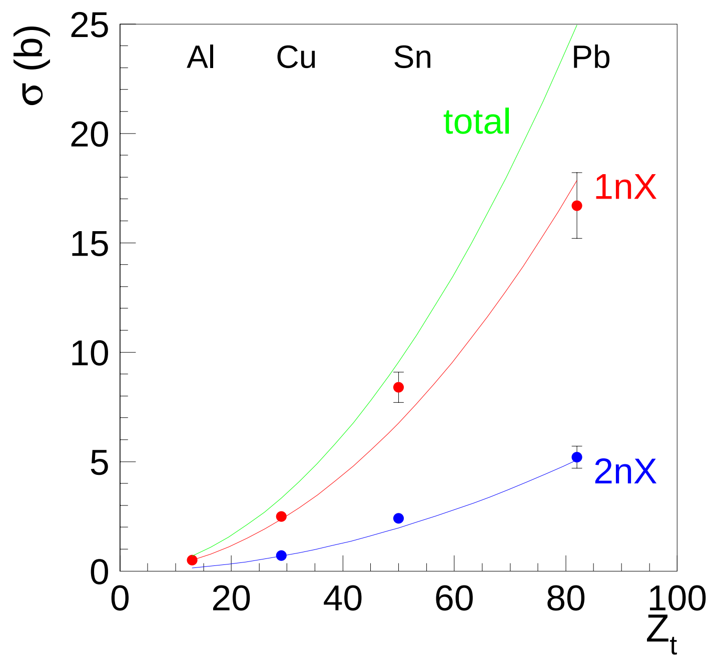

Left: ^{28}Si(γ,tot) as recorded in the FLUKA database, 8 interval Bezier fit as used for the Electromagnetic Dissociation event generator.

Right: calculated total, $1nX$ and $2nX$ electromagnetic dissociation cross sections for 30 A GeV Pb ions on Al, Cu, Sn and Pb targets. Points - measured cross sections of forward $1n$ and $2n$ emission as a function of target charge (M. B. Golubeva et al., in press)

158 GeV/n fragmentation

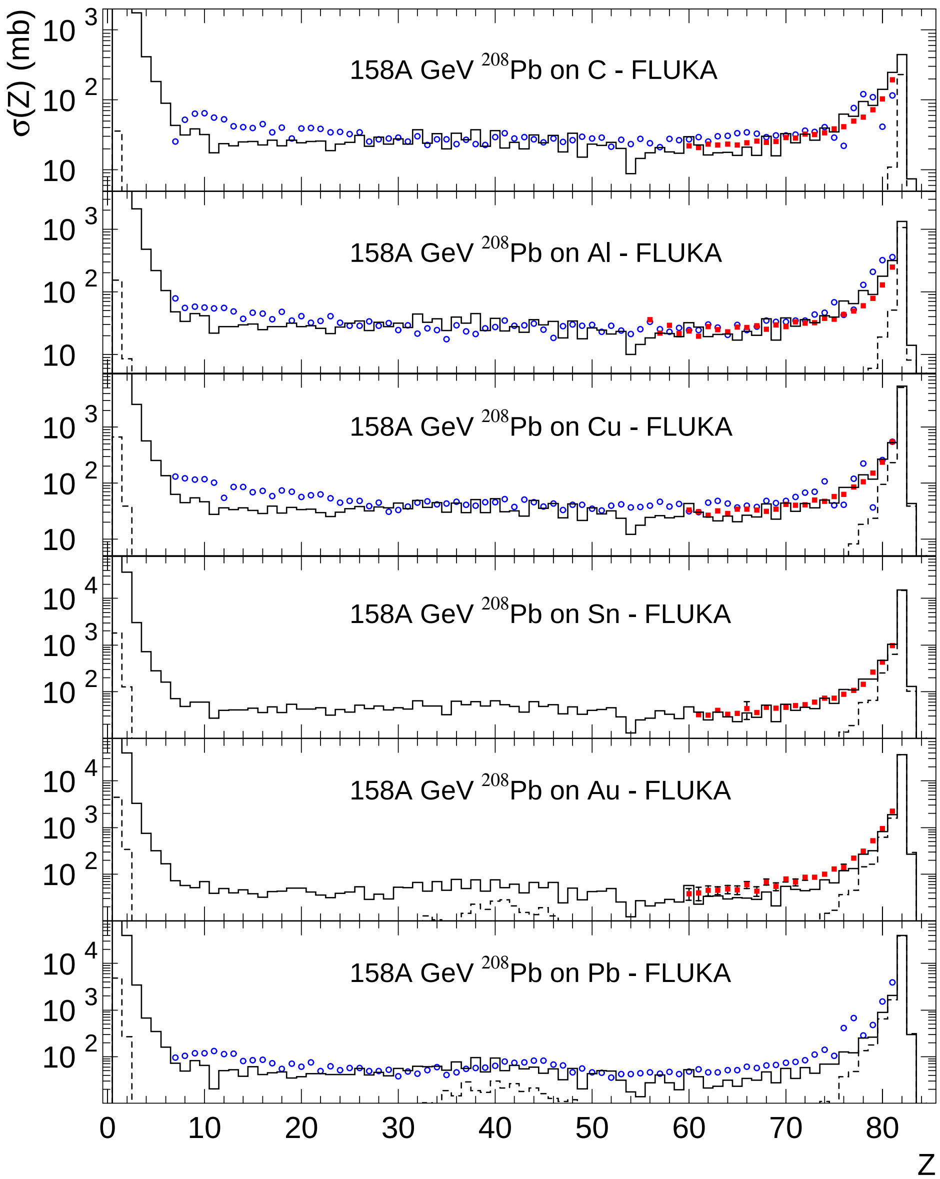

Fragment charge cross sections for 158 AGeV Pb ions on various targets. Data (symbols) from NPA662, 207 (2000), NPA707, 513 (2002) (blue circles) and from C. Scheidenberger et al PRC, in press (red squares), histos are FLUKA (with DPMJET-III) predictions: the dashed histo is the electromagnetic dissociation contribution

Future

★ Evaporation/fragmentation, residual nuclei:

- Further development of the new model
- Extended benchmarks against real life accelerator environment activation

★ Particle (particularly pion) production at few GeV's

- Refined resonance production and reinteraction model
- "Normal" to Glauber cascade transition

★ Rich development program for ions for the future:

- New QMD (Milan+Houston) model in place of the modified rQMD-2.4 for intermediate energies
- BME model (from Milan University, see F.Cerutti talk at this Conference) covering the low energy range

This work was partially supported under:

- NASA Grants: NAG8-1658 and NAG8-1901
- DOE contract DE-AC02-76SF00515
- ASI Contract I/R/320/02
- European Union contract no. FI6R-CT-2003-508842, "RISC-RAD"

From resonance production to DPM

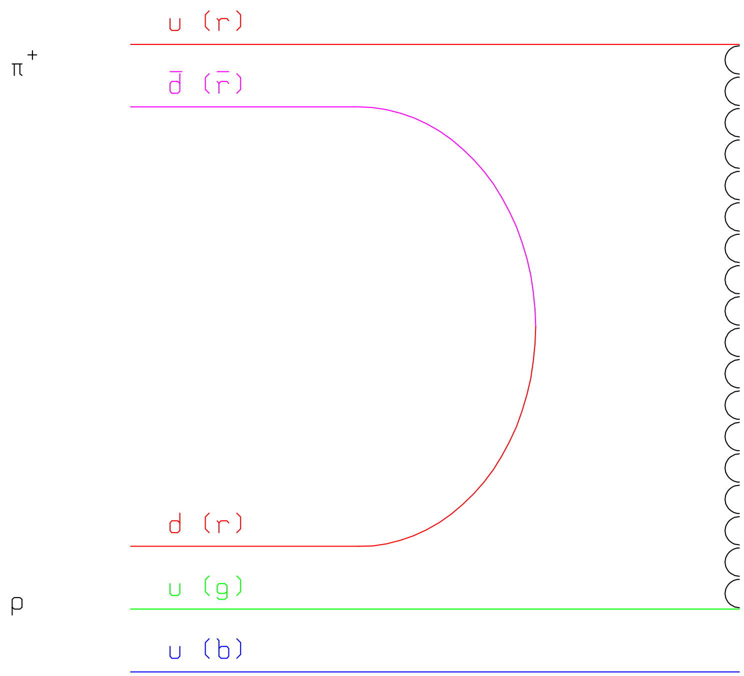

Single chain diagram for $\pi^+ - p$ scattering, corresponding to a physical particle exchange. The color (red, blue, and green) and quark combination shown in the figure is just one of the allowed possibilities

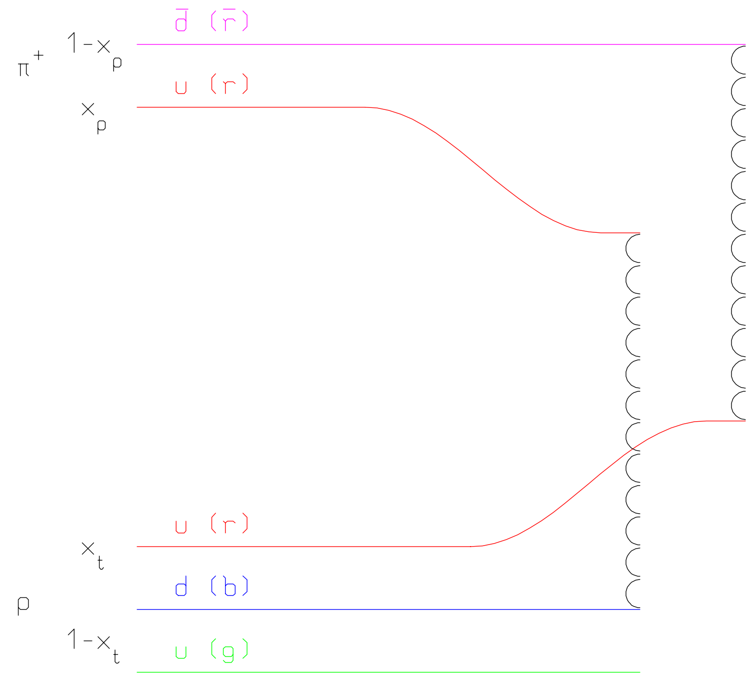

Leading two-chain diagram in DPM for $pi^+ - p$ scattering. The color (red, blue, and green) and quark combination shown in the figure is just one of the allowed possibilities

DPM: chain examples

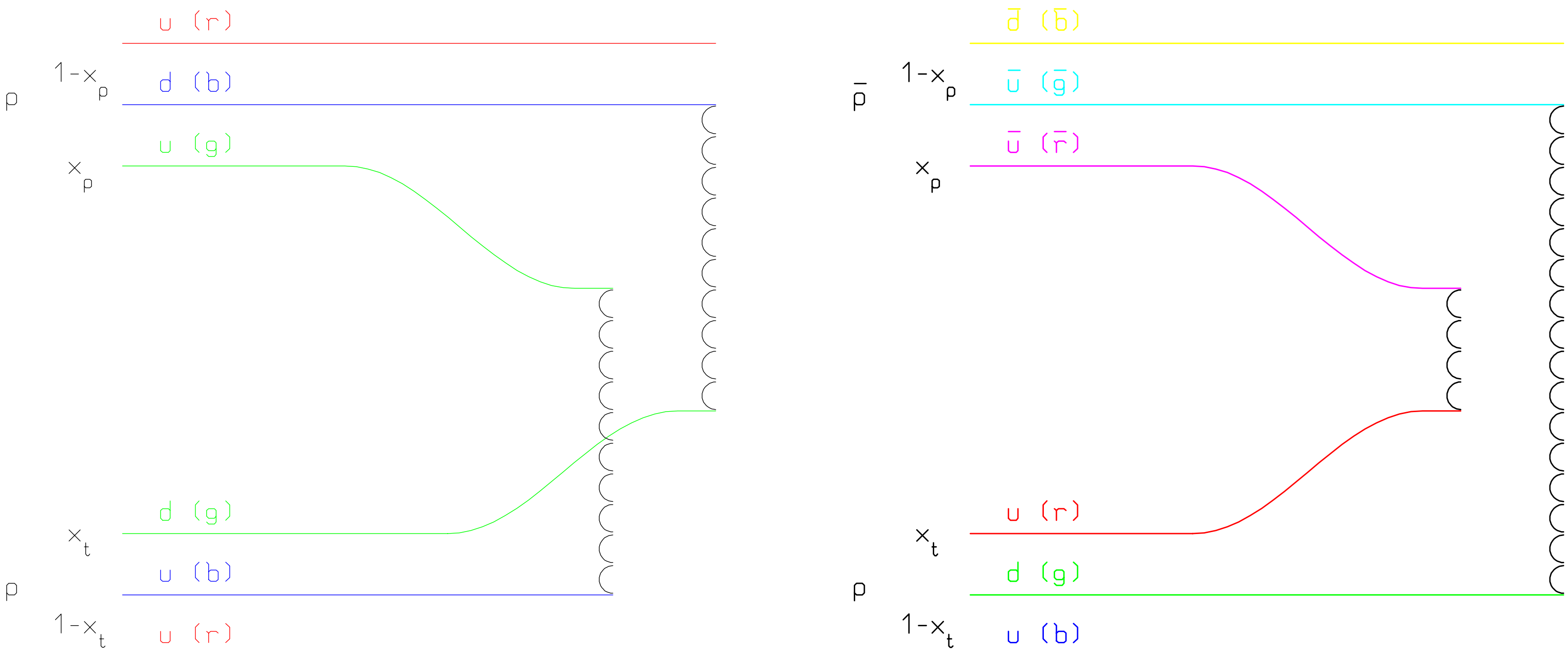

Leading two-chain diagrams in DPM for $p - p$ (left) and $\bar{p} - p$ (right) scattering. The color (red, blue, and green) and quark combinations shown in the figure are just one of the allowed possibilities

Nonelastic hN high E: (K$^-$p) , (π^-p) 10-16 GeV, p$_T$

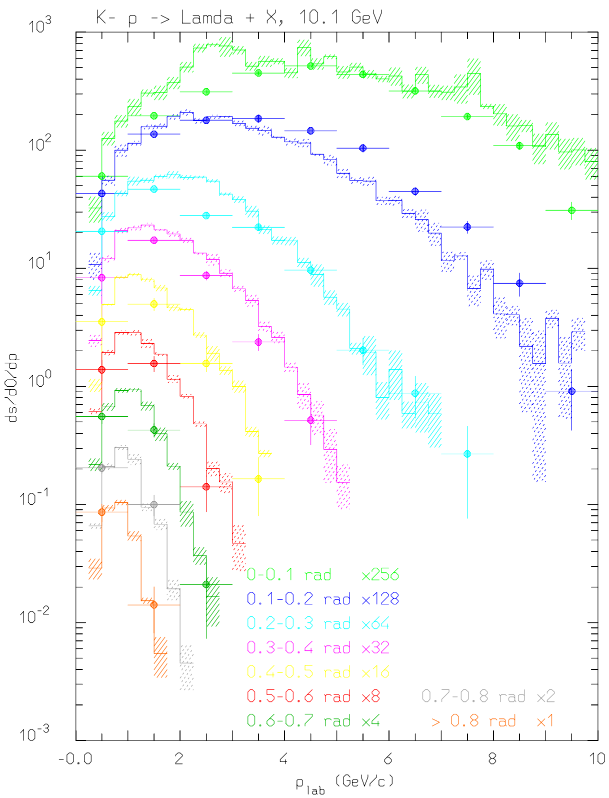

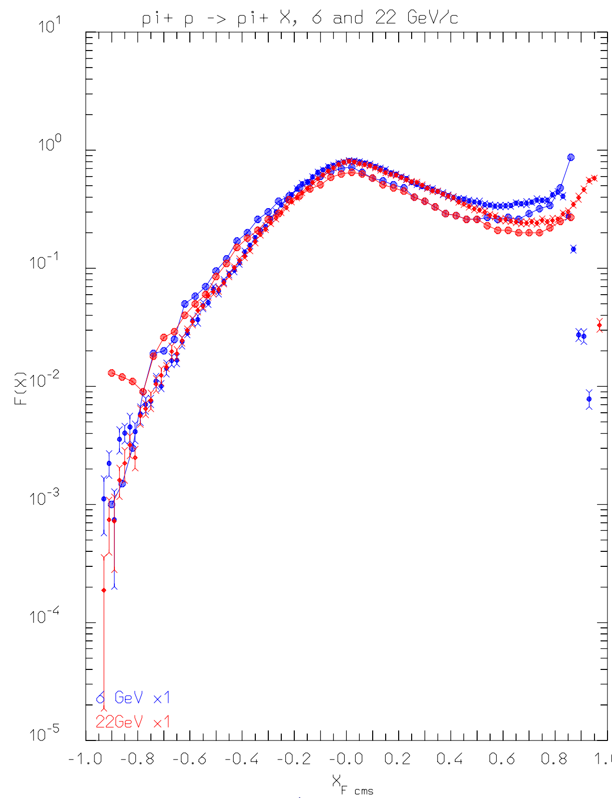

Left: Double differential cross section for K$^-$p $\rightarrow \Lambda X$ at 10 GeV/c. Right: Invariant σ spectra, as a function of Feynman x_F^*, for π^+ emitted from (π^+,p) at various momenta. Data from M.E Law et al. LBL80 (1972).

Nonelastic hN high E: (π^+ p) 250GeV, x_F and p_t

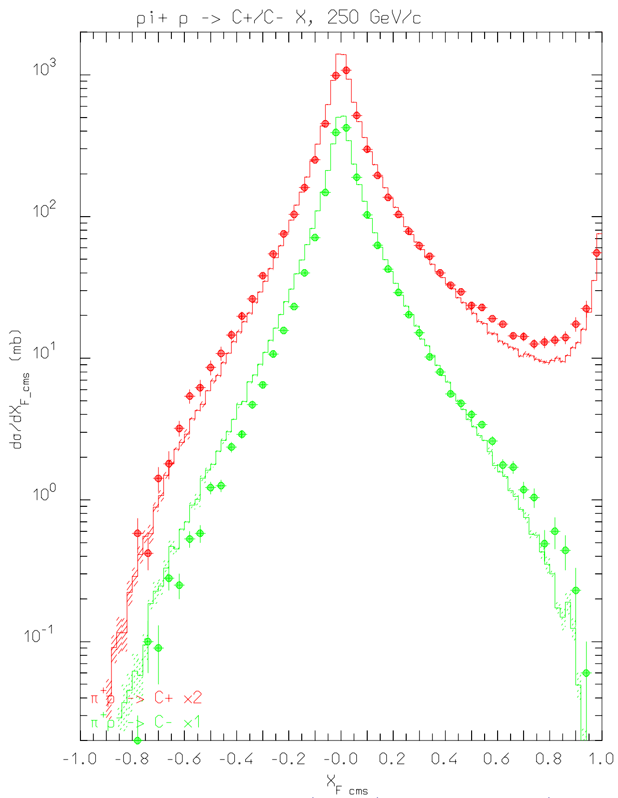

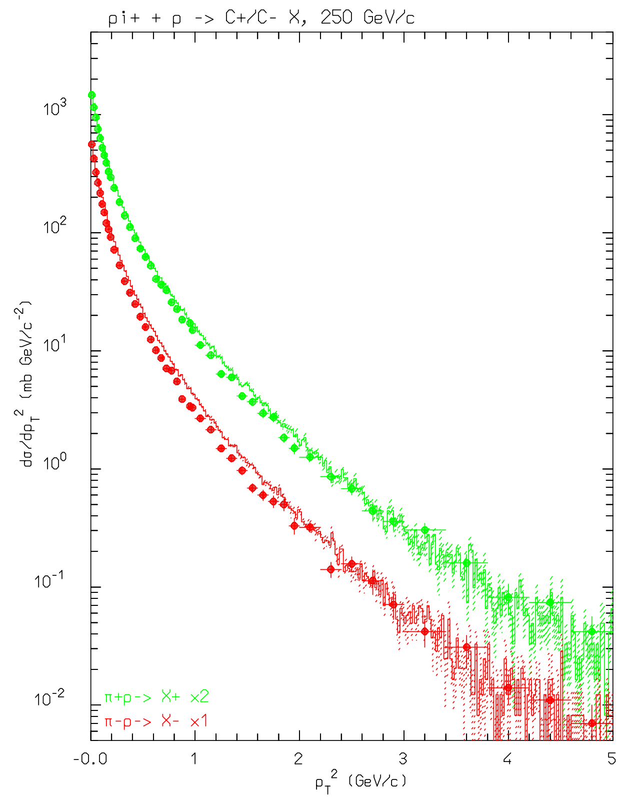

Feynman x_F^* (left) and p_t (right) spectra of positive particles and π^- produced by 250 GeV/c π^+ incident on an hydrogen target. Exp. data (symbols) have been taken from M. Adamus et al. ZPC39, 311 (1988).

h-A at high energies: Glauber-Gribov

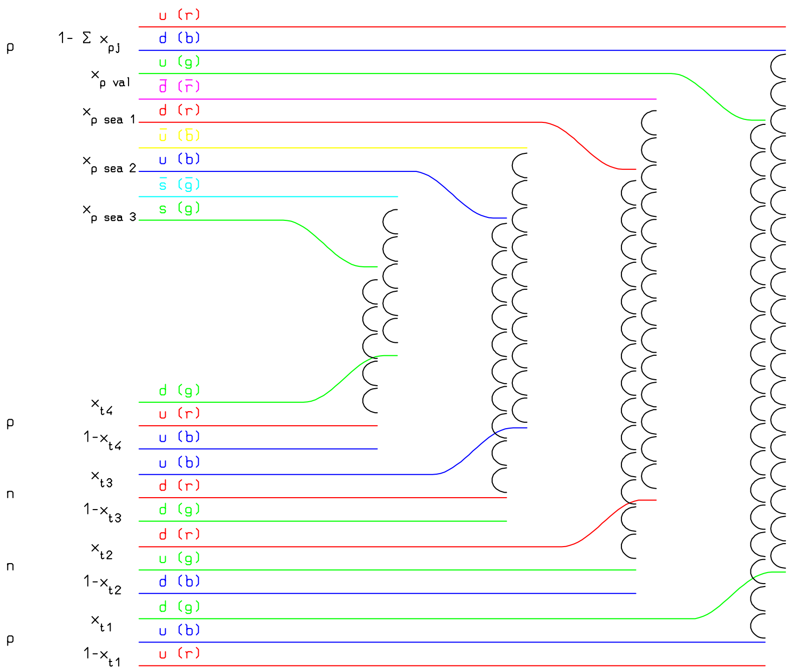

One of the possibilities for Glauber-Gribov scattering with 4 collisions

Gribov

$\Downarrow$

2ν chains

2 valence-valence chains

$2(\nu - 1)$ chains between projectile sea and target valence (di)quarks.

No freedom, except in mass effects at low energies.

Fermi motion included $\rightarrow$ smearing of E and p_T distributions

Nonelastic hA interactions at high energies: examples

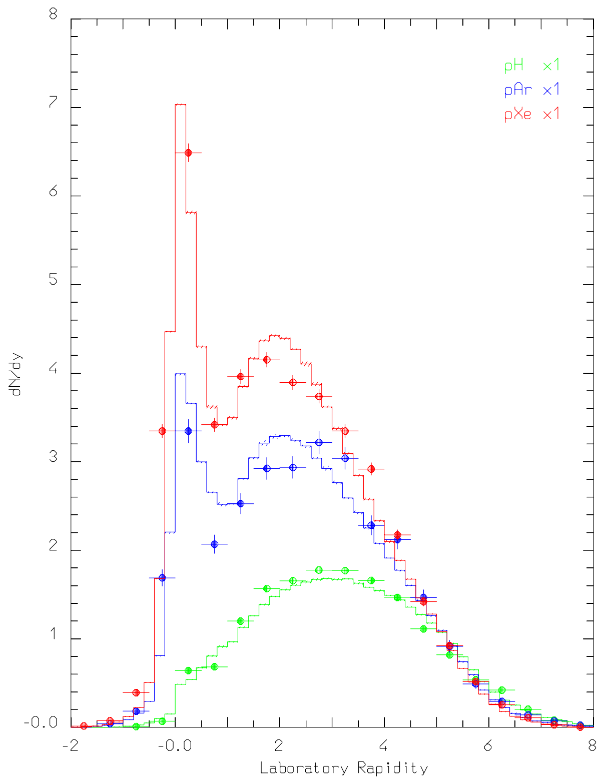

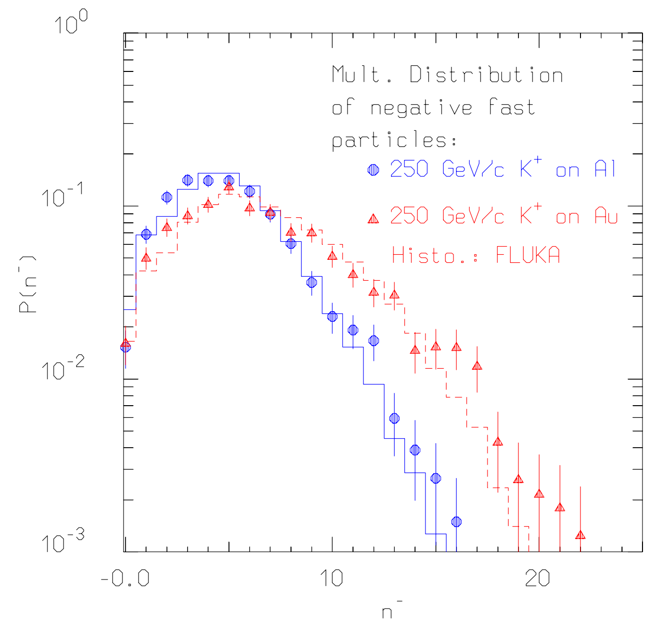

Rapidity distribution of charged particles produced in 200 GeV proton collisions on Hydrogen, Argon, and Xenon target (left), and multiplicity distribution of negative shower particles for 250 GeV/c K^+ on Aluminium and Gold targets (right). Data from C. De Marzo et al., PRD26, 1019 (1982), I.V. Ajinenko et al. ZPC42 377 (1989).

Transverse momentum in ν interactions

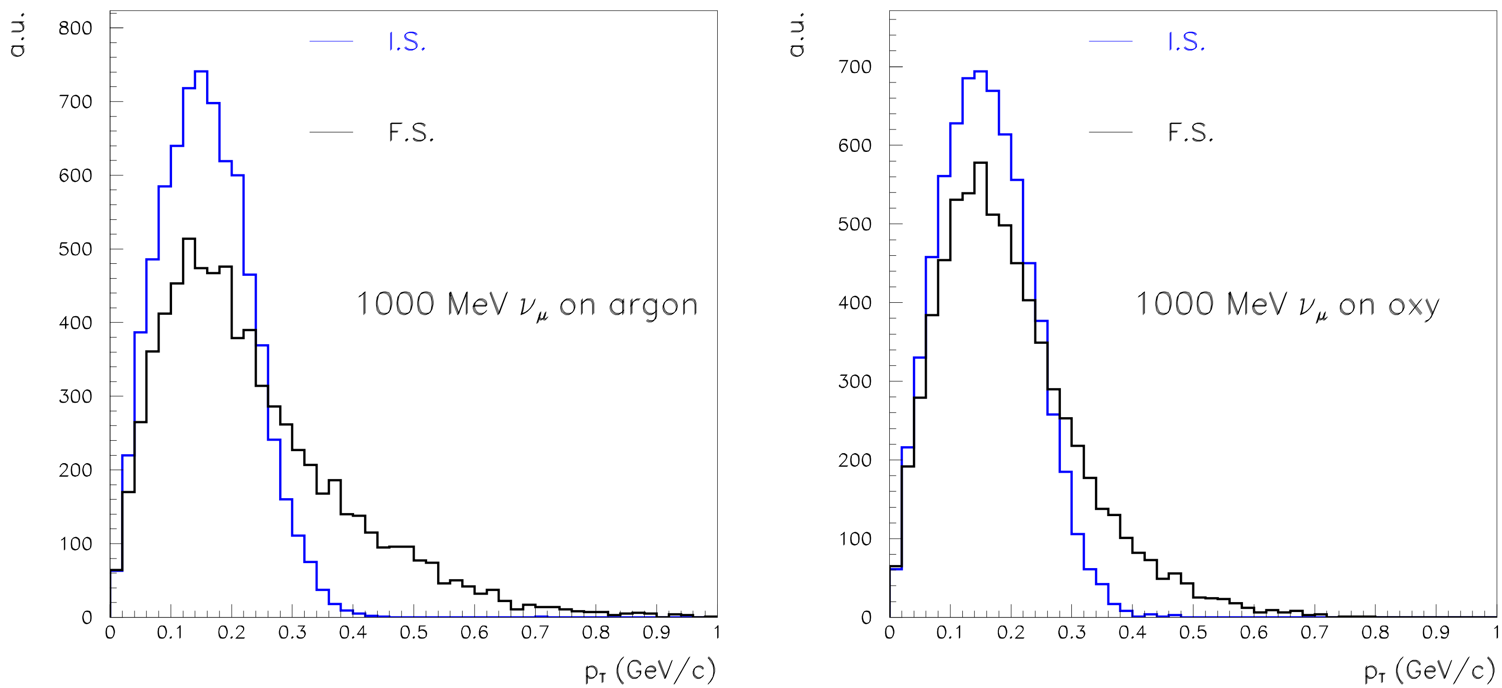

Total momentum of "detectable" reaction products (i.e. no residual nucleus) in the plane$\perp$ to the beam axis

At low E_ν is dominated by Fermi, but reinteractions are important

QE E_ν reconstruction

QE : "golden" channel for kinematic reconstruction, expecially in Water Cherenkov detectors (like Kamiokande). ν energy reconstructed from lepton momentum and angle, but:

initial state distortion

contaminations from other reaction channels, ex. pion production followed by pion absorption

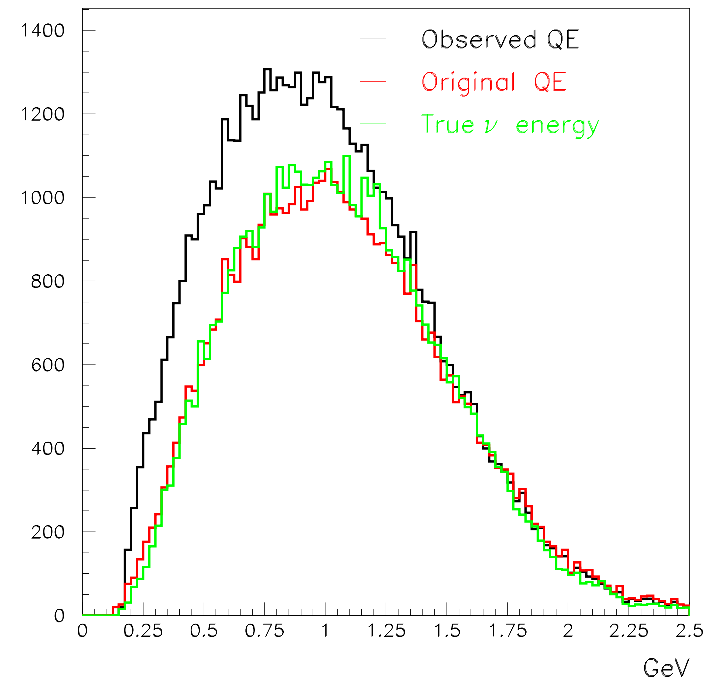

Example: reconstruction of the MiniBoone (Booster neutrino experiment at Fermilab) spectrum from "QE" interactions in water

Pion absorption cross sections: examples

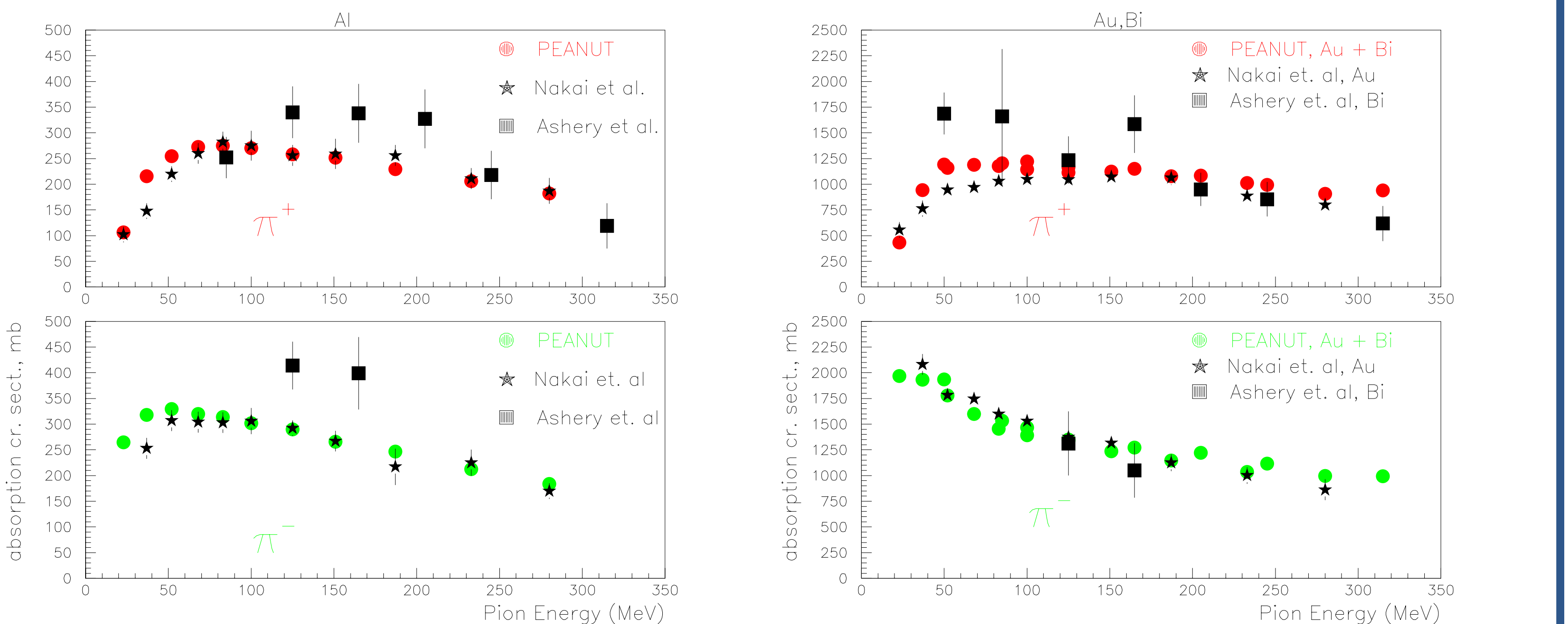

Computed and experimental pion absorption cross section on Aluminium as a function of energy

Computed and experimental pion absorption cross section on Gold or Bismuth as a function of energy

(Exp. data: D. Ashery et al., **PRC23**, (1981) 2173 and K. Nakai et. al., **PRL44**, (1979) 1446)

Pion-nucleus interactions: examples

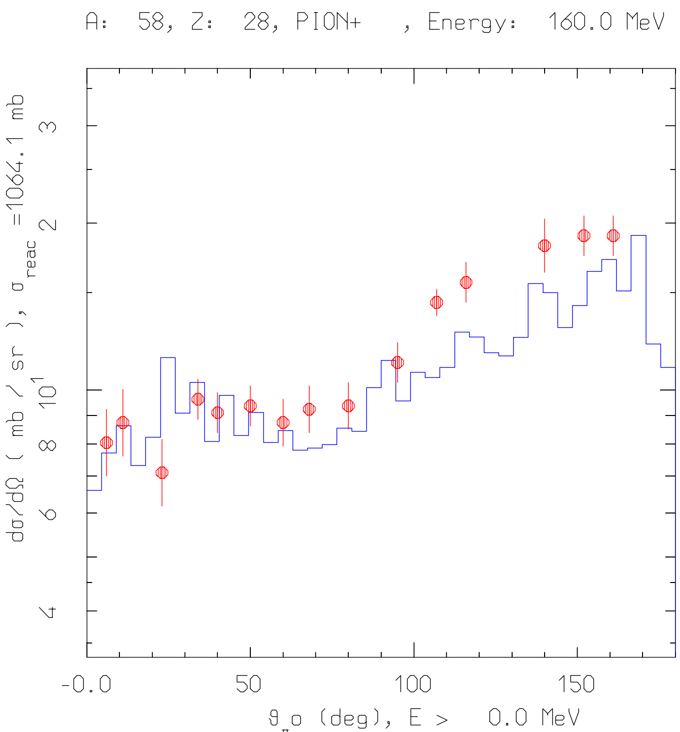

Computed and experimental pion charge exchange angular distribution for ^{58}Ni(π^+,π^0) at 160 MeV

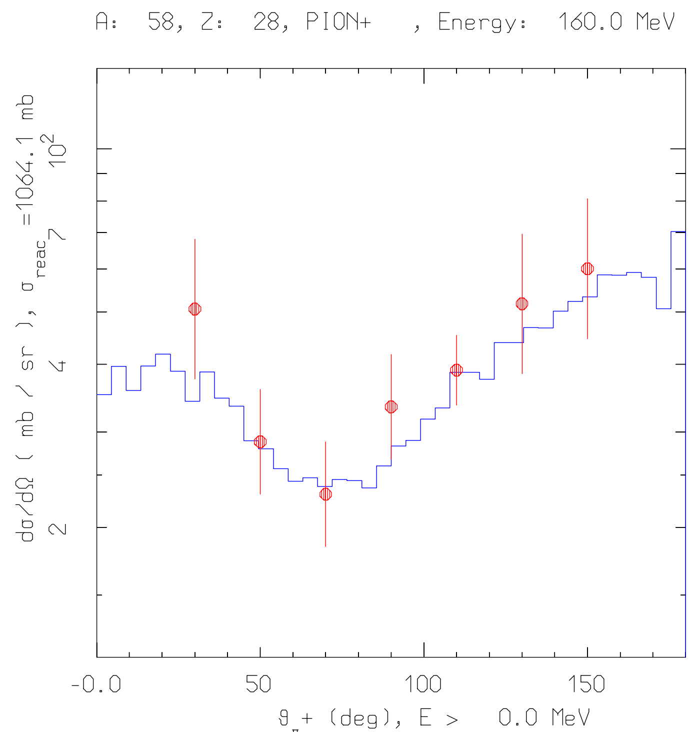

Computed and experimental pion inelastic angular distribution for ^{58}Ni$(\pi^+,\pi^{+'})$ at 160 MeV

Experimental data: Burger et al., **PRC41**, (1990) 2215 and McKeown et al., **PRC24**, (1981) 211

Nucleon emission: thin target examples I

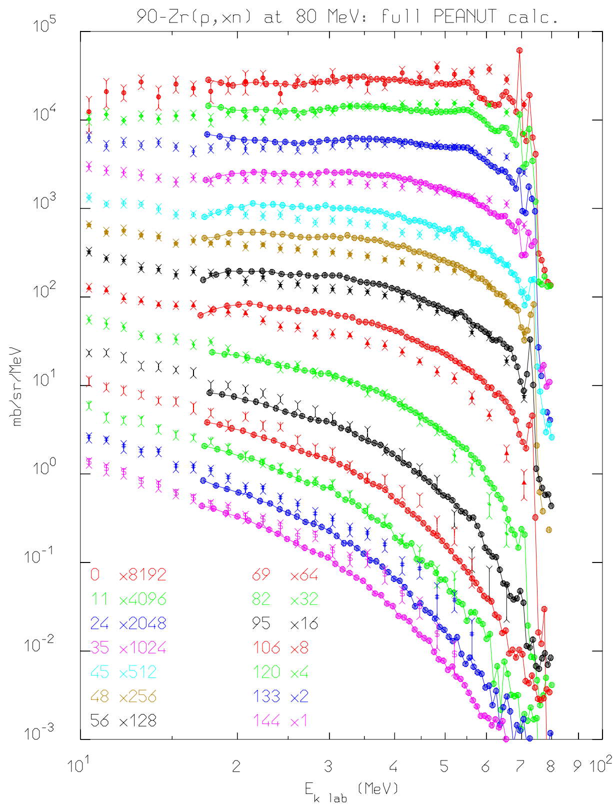

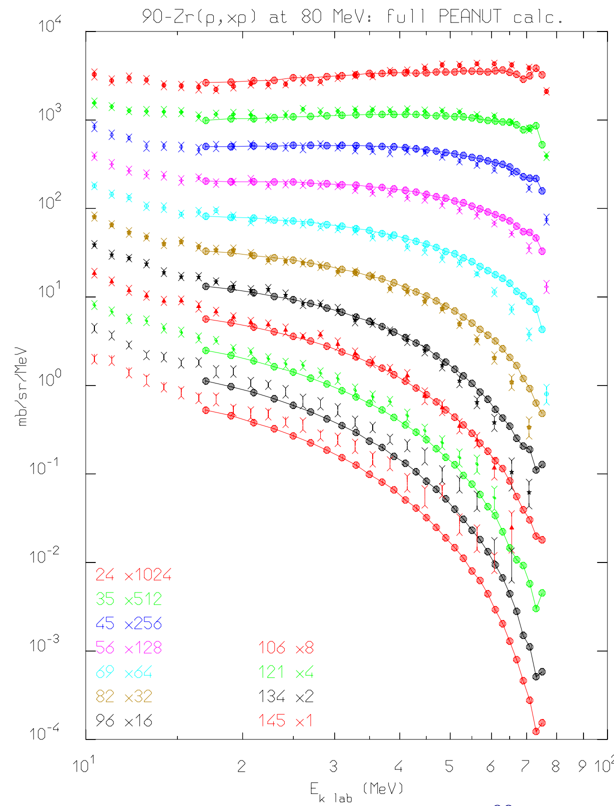

Computed (light symbols) and experimental (symbols with lines) double differential distributions for ^{90}Zr(p,xn) (left) and ^{90}Zr(p,xp) at 80.5 MeV. The exp. data have been taken from M.Trabandt et al. **PRC39** (1989) 452 and A.A. Cowley et al., **PRC43**, (1991) 678

Nucleon emission: thin target examples I

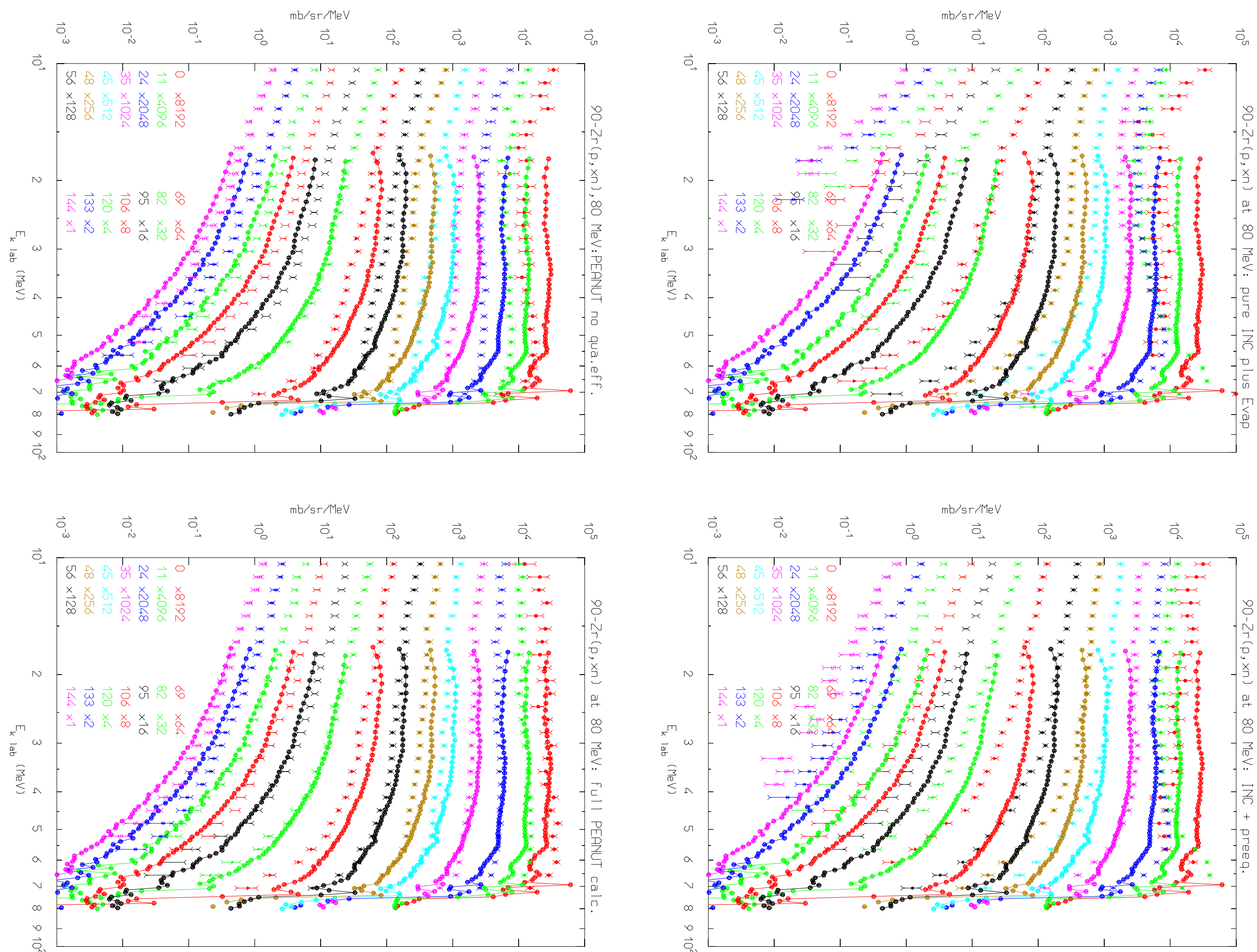

Nucleon emission: thin target examples I

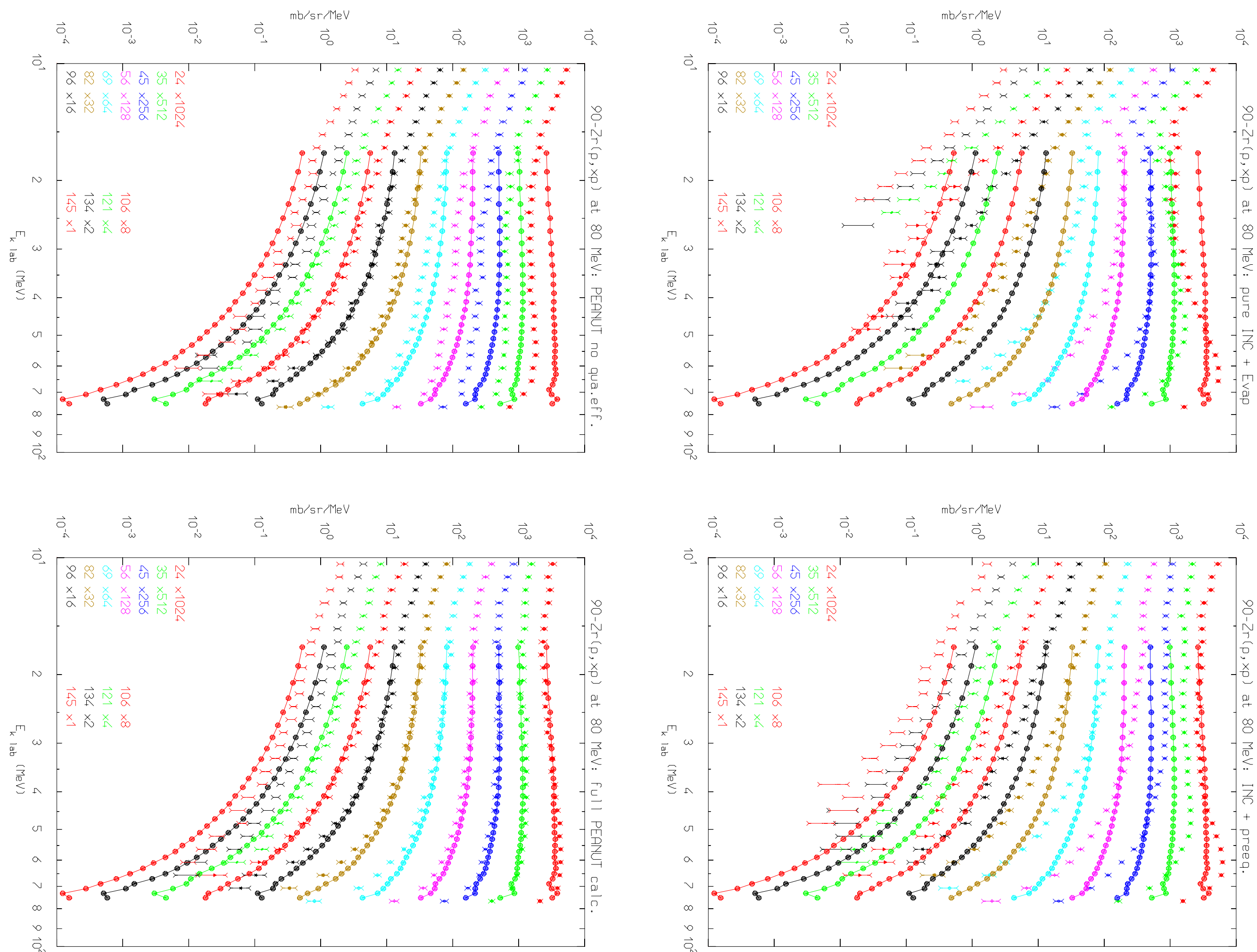

CERN activation benchmark: Aluminium

Table 2: Al, cooling times 1d 16h, 16d 08h , 51d 09h

Isotope	$t_{1/2}$	Exp Bq/g	± %	STD FLUKA/Exp	± %	NEW FLUKA/Exp	± %
Be 7	53.29d	0.789	13	0.364	16	0.688	19
Na 22	2.60y	0.365	9.6	0.841	11	0.752	11
Na 24	14.96h	38.6	3.6	0.854	4.0	0.815	4.6
Sc 44	3.93h	0.229	24	2.219	27	0.820	36
Sc 46	83.79d	0.025	16	1.571	19	0.902	28
Sc 47	80.28h	0.163	12	0.986	27	(1.486	43)
V 48	15.97d	0.199	7.4	0.931	18	(0.938	29)
Cr 51	27.70d	0.257	17	0.873	23	0.942	28
Mn 52	5.59d	0.224	5.6	2.369	9.6	0.936	24
Mn 54	312.12d	0.081	11	0.972	15	0.917	19
Co 57	271.79d	0.00424	32	0.833	50	(0.760	67)
Co 58	70.82d	0.019	22	1.820	27	0.841	39

CERN activation benchmark: Cu

Table 3: Cu, cooling times 34m, 1h 07m, 48d 3h 21m

Isotope	$t_{1/2}$	Exp Bq/g	± %	STD FLUKA/Exp	± %	NEW FLUKA/Exp	± %
Be 7	53.29d	1.29	13	0.045	17	1.472	14
Na 22	2.60y	0.029	14	0.655	17	0.677	20
Na 24	14.96h	14.8	8.5	0.266	10	0.515	12
K 42	12.36h	21.6	15	0.592	17	0.685	17
K 43	22.30h	6.38	11	0.656	14	0.844	16
Sc 43	3.89h	24.6	24	0.645	25	0.443	27
Sc 44	3.93h	45.4	9.5	1.160	10	0.863	10
Sc 46	83.79d	0.865	8.3	0.890	9.0	0.850	9.7
Sc 47	80.28h	11.0	14	0.927	16	0.959	17
Sc 48	43.67h	3.16	13	1.151	16	1.293	16
mSc 44	58.60h	18.4	13	1.280	14	0.952	14
V 48	15.97d	1.12	7.8	1.647	8.4	1.220	9.0
Cr 49	42.30m	15.0	25	1.357	26	0.909	27
Cr 51	27.70d	3.55	13	1.306	13	1.099	14
Mn 52	5.59d	18.3	5.5	0.790	6.3	0.651	6.9
mMn 52	21.10m	9.16	33	1.940	34	1.616	35
Mn 54	312.12d	1.13	10	1.177	11	1.171	11
Mn 56	2.58h	27.7	5.8	0.784	7.1	0.872	8.0

CERN activation benchmark: Cu cont.

Table 4: Cu, cooling times 34m, 1h 07m, 48d 3h 21m

Isotope	$t_{1/2}$	Exp Bq/g	± %	STD FLUKA/Exp	± %	NEW FLUKA/Exp	± %
Fe 59	44.50d	0.558	10	0.699	12	0.761	14
Co 55	17.53h	7.41	10	0.855	12	0.712	14
Co 56	77.27d	1.20	7.2	1.161	8.1	1.057	8.6
Co 57	271.79d	1.75	9.9	0.917	10	0.851	11
Co 58	70.82d	6.51	10	0.889	10	0.895	11
Co 60	5.27y	0.172	8.5	0.798	8.9	0.832	9.4
Co 61	99.00m	52.7	12	0.836	13	0.878	14
Ni 57	35.60h	4.78	12	0.864	15	0.789	16
Ni 65	2.52h	3.46	19	1.553	22	1.350	24
Cu 60	23.70m	16.4	8.7	0.847	9.9	0.787	11
Cu 61	3.33h	165.	27	1.047	28	0.944	28
Cu 64	12.70h	595.	13	0.564	14	0.560	15
Zn 62	9.19h	5.66	20	1.213	22	1.117	24
Zn 65	244.26d	0.117	12	0.635	14	0.615	17

CERN benchmark: residual dose rates

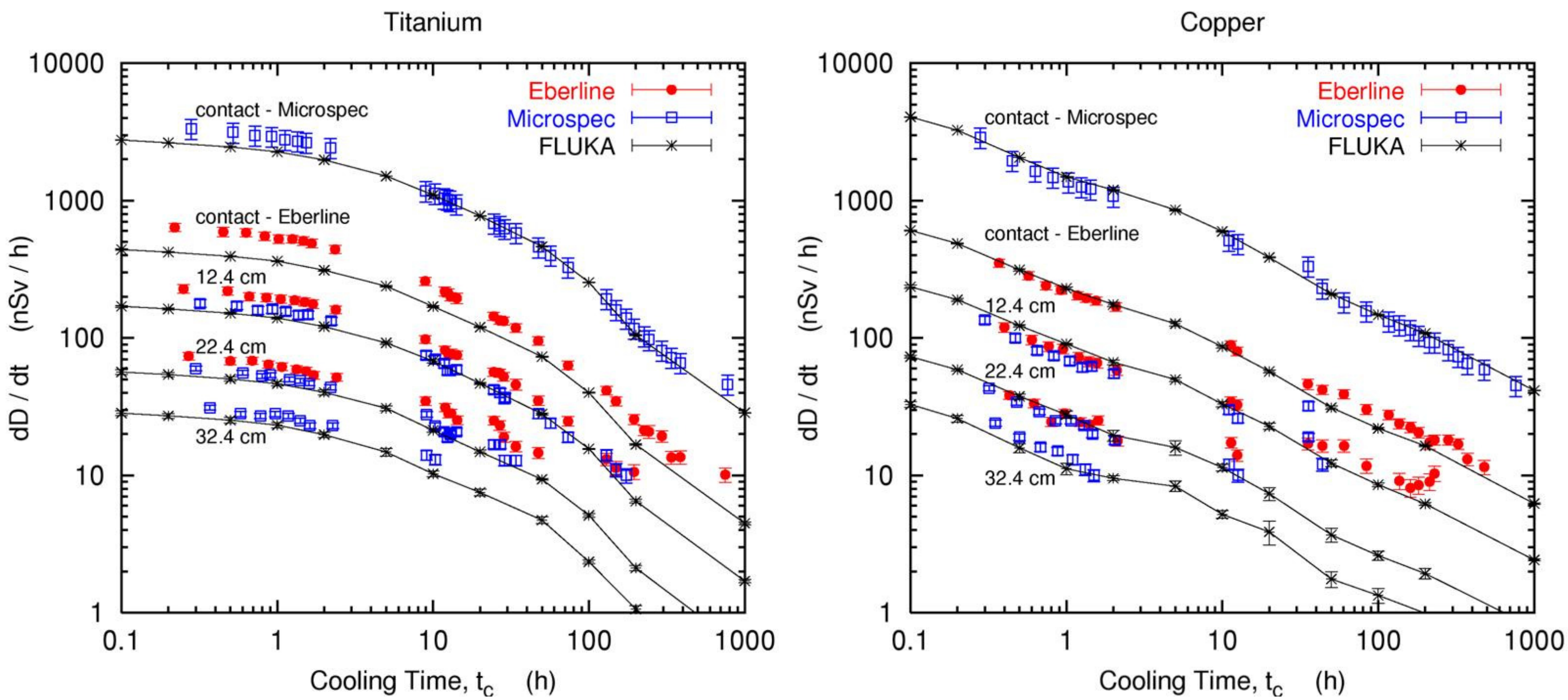

Measured (blue and red symbols, two different instruments), and simulated residual dose rates as a function of time (see M. Brugger et al, Proc. ICRS10 in press, for a thorough discussion of the exp. and simulation methodology).
Left: Titanium target — Right: Copper target

CERN benchmark: residual dose rates

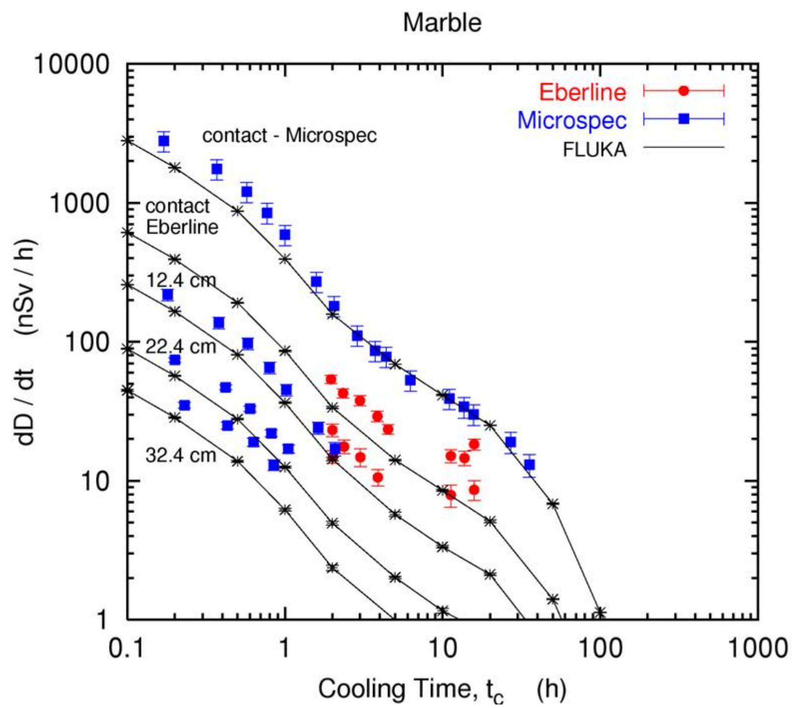

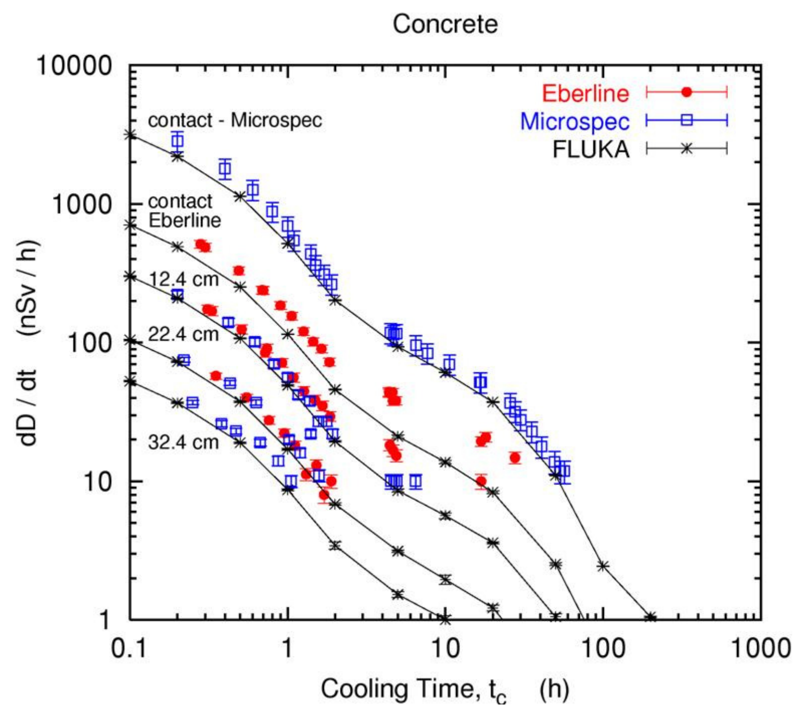

Measured (blue and red symbols, two different instruments), and simulated residual dose rates as a function of time (see M. Brugger et al, Proc. ICRS10 in press, for a thorough discussion of the exp. and simulation methodology).
Left: Marble target — Right: Concrete target

In-Medium cross sections: example cont.

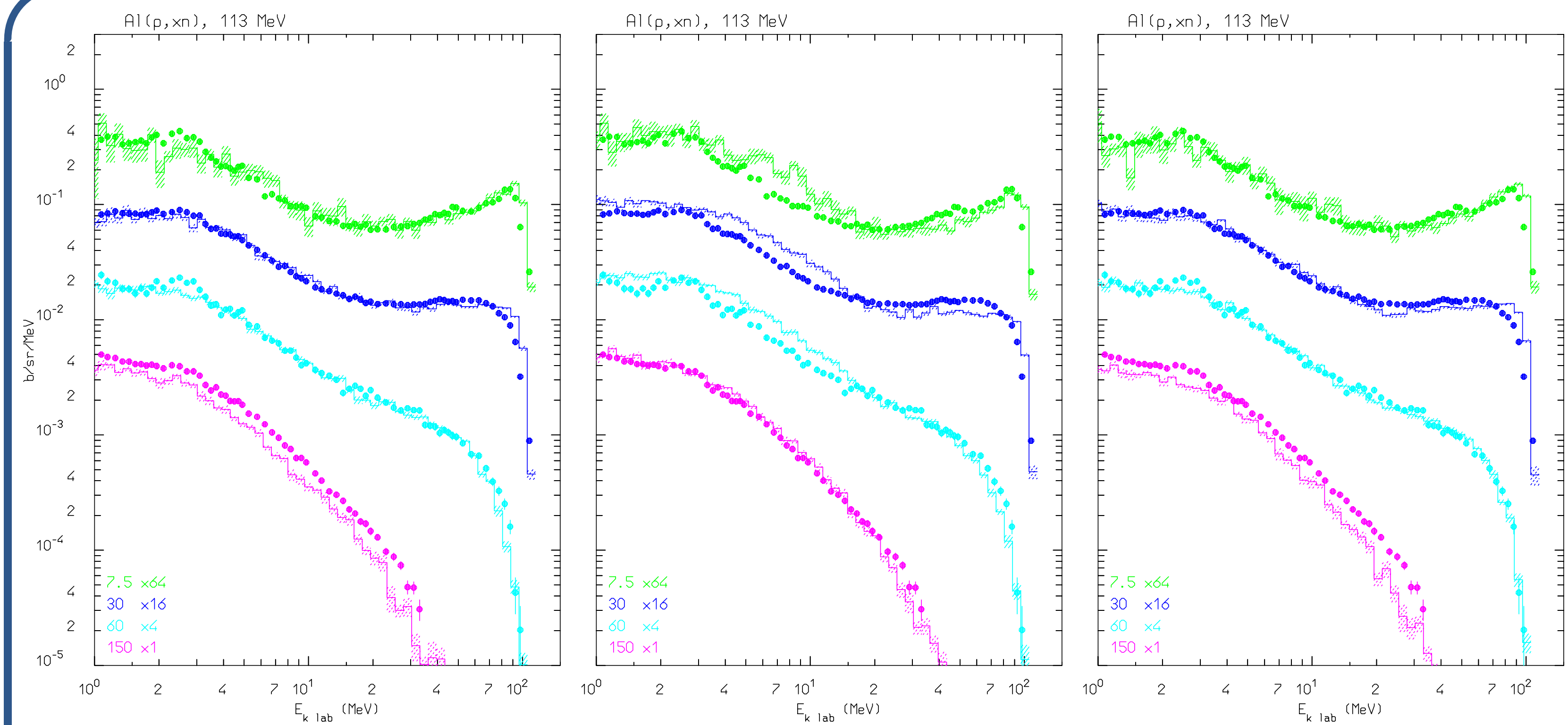

Double differential neutron distributions for Al(p,xn) at 113 MeV. “Normal” PEANUT (left), PEANUT with coherence length, correlation length, and nucleon hard core effects switched off (center), PEANUT with in-medium cross sections and coherence length, correlation length, and nucleon hard core effects switched off (right). Histograms: computed with FLUKA; symbols: experimental data from Meier et al, Nucl. Sci. Eng. **102** (1989), 310

FLUKA with modified RQMD-2.4 (cascade mode)- results

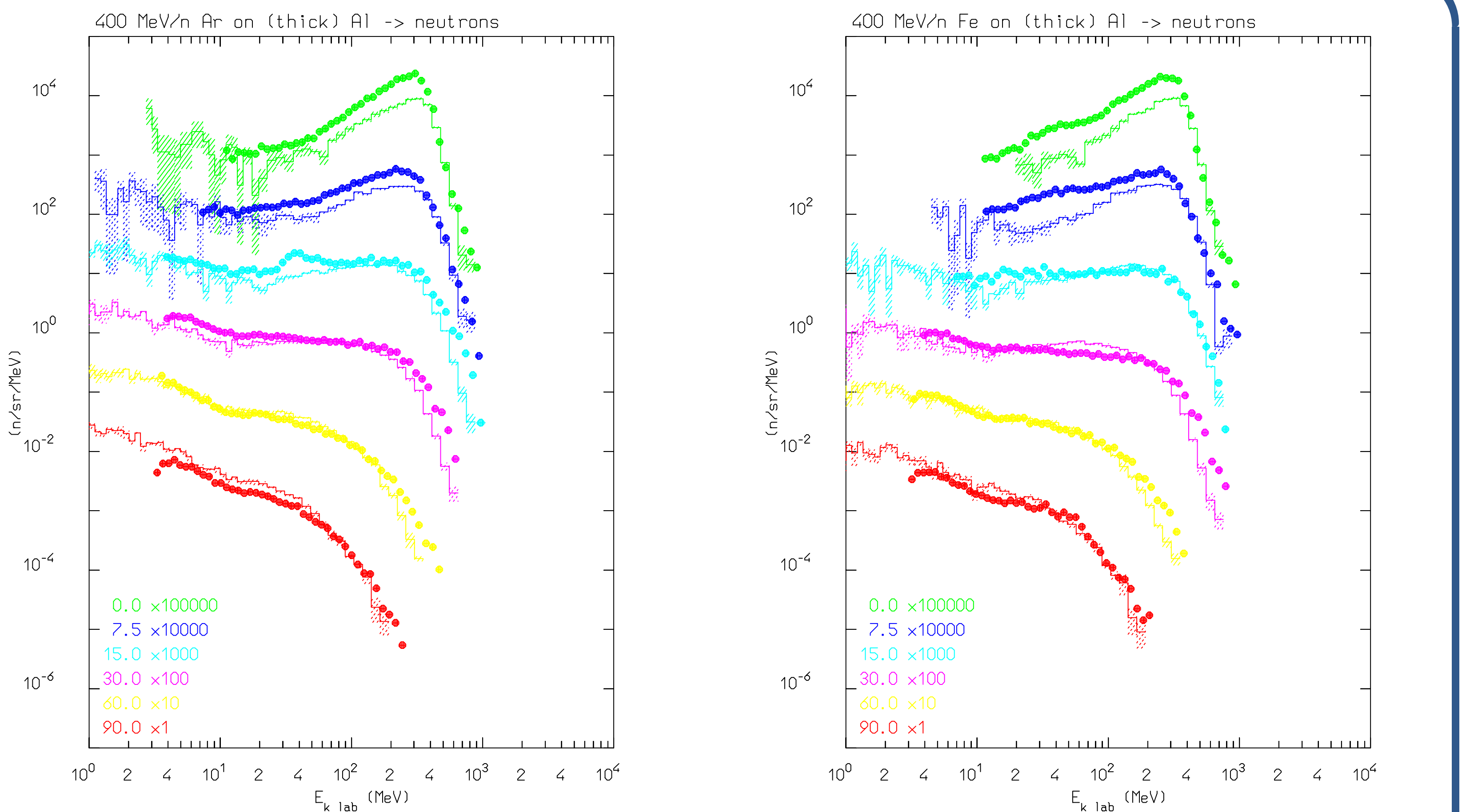

Double differential neutron yield by 400 MeV/n Ar (left) and Fe (right) ions on thick Al targets, histo FLUKA, dots exp. data (PRC62 044615 (2000)).

10.6 GeV/n fragmentation

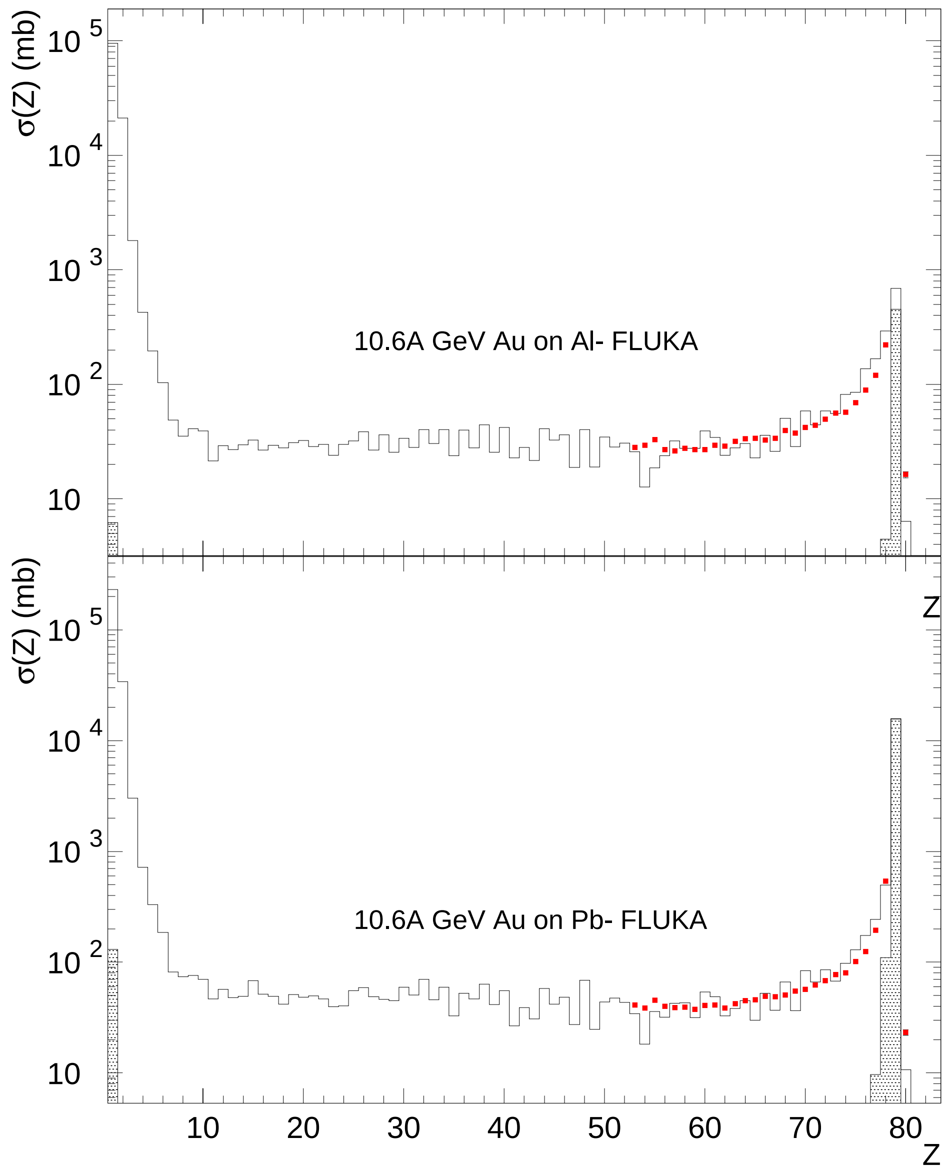

Fragment charge cross sections for 10.6 AGeV Au ions on Aluminium and Lead. Data (symbols) from PRC52, 334 (1995), histos are FLUKA (with DPMJET-III) predictions: the hatched histo is the electromagnetic dissociation contribution

Thick target neutron production: examples

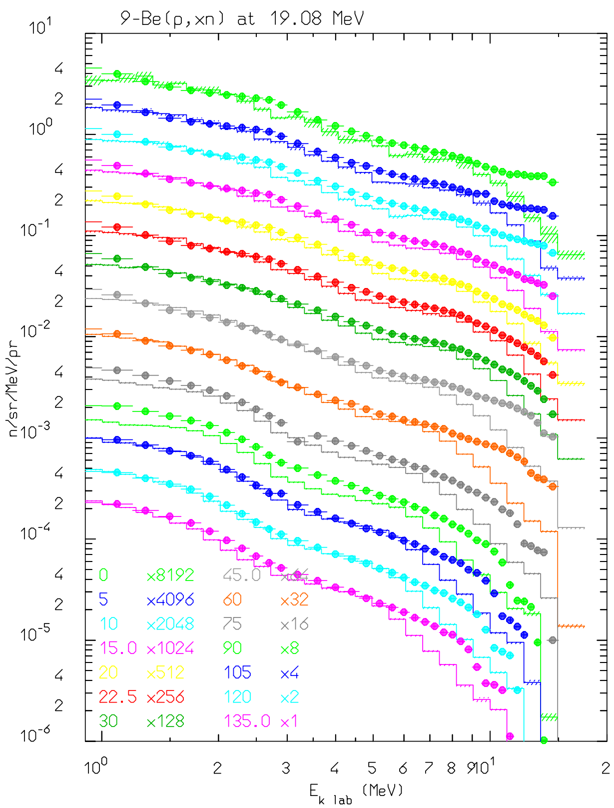

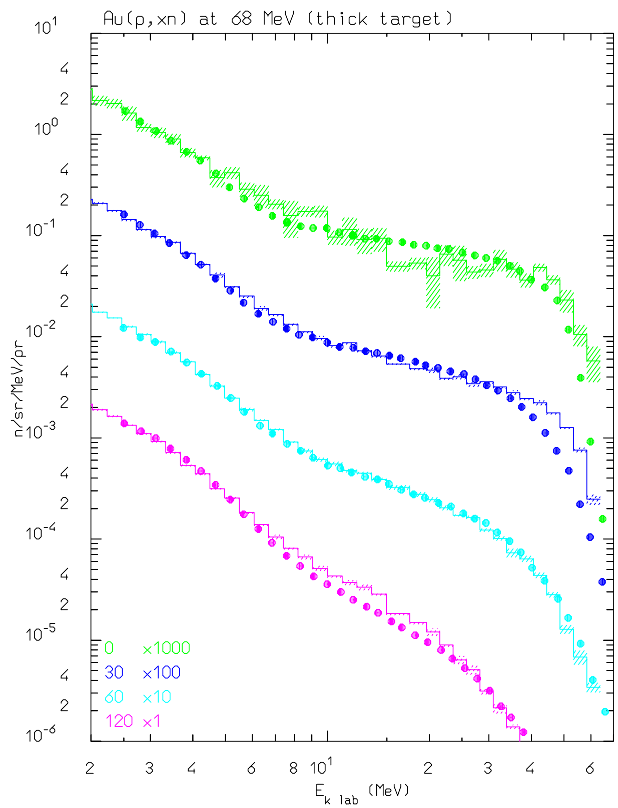

Simulated (dashed histogram) and experimental (symbols) neutron double differential distributions out of stopping length targets for 19.08 MeV protons on beryllium (left, H.J. Brede et. al., **NIMA274** (1989) 332) and 68 MeV protons on gold (right, S. Meigo et al., NDST97)

Thick target neutron production: examples II

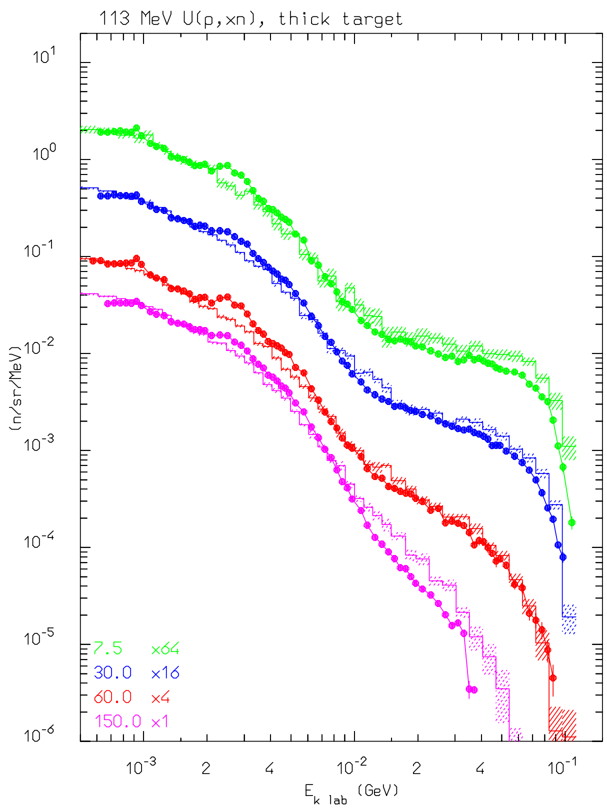

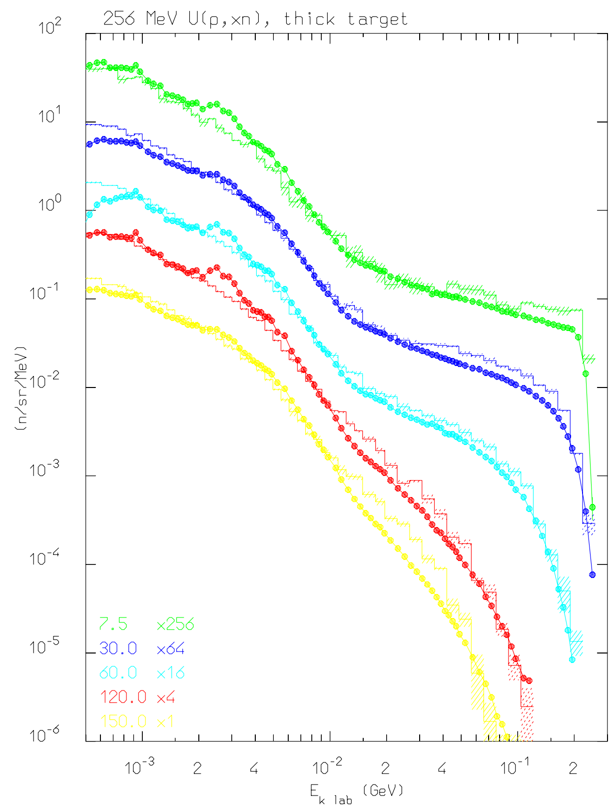

Simulated (dashed histogram) and experimental (symbols) neutron double differential distributions out of stopping length targets for 113 (left, M.M. Meier et al., Nucl. Sci. Eng. **110**, (1992) 299) and 256 MeV protons on uranium (right, M.M. Meier et al., Nucl. Sci. Eng. **102**, (1989) 310)

Thick target neutron production: examples III

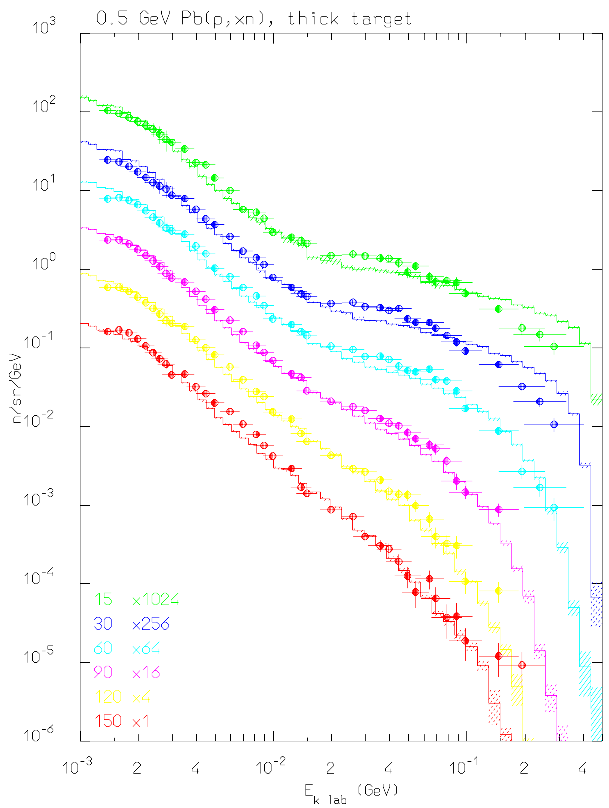

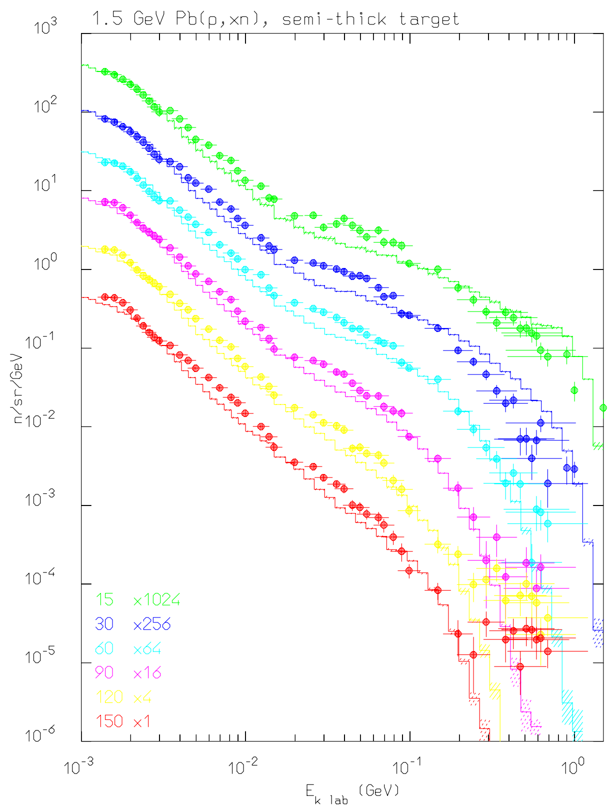

Simulated (dashed histogram) and experimental (symbols) neutron double differential distributions out of (semi)stopping length targets for 500 (left) and 1500 MeV protons on lead (right). Exp. data from S. Meigo et al., JAERI-Conf 95-008, (1995), 213

Neutron production: TARC

Experiment

Protons from the CERN PS , 2.5 or 3.57 GeV/c

Lead target , 334 ton , 99.99% purity

64 Instrumentation holes, different detectors to measure neutrons from thermal to MeV

Simulations: EA MC

Spallation production, transport down to 20 MeV : FLUKA

Neutron transport and interactions below 20 MeV and target evolution: new code EA-MC (C.Rubbia et al)

Refs.: PLB458 (1999) 167, NIMA478 (2002) 577

Neutron production examples: TARC (PLB458 167, NIMA478 577)

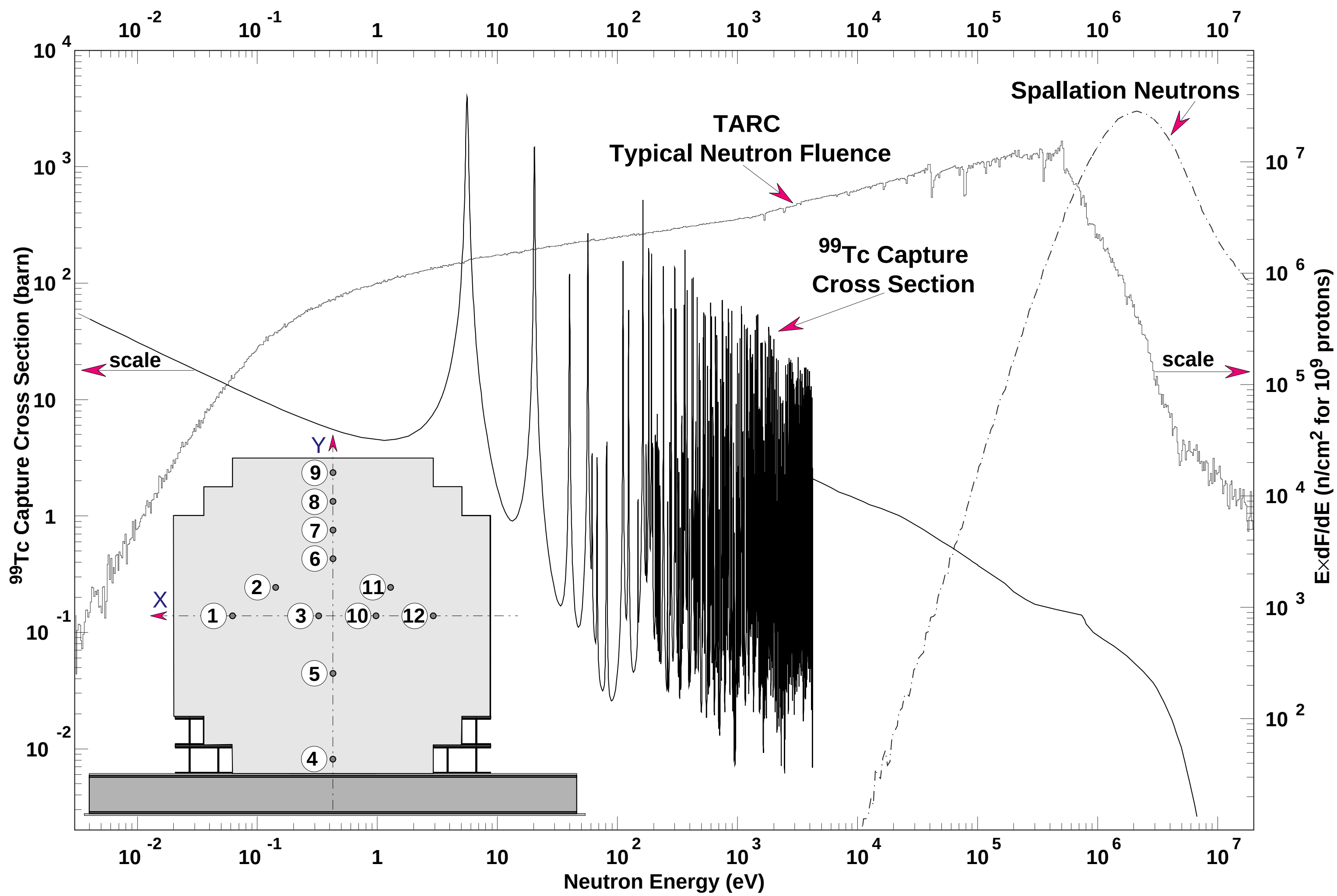

Neutron production examples: TARC (PLB458 167, NIMA478 577)

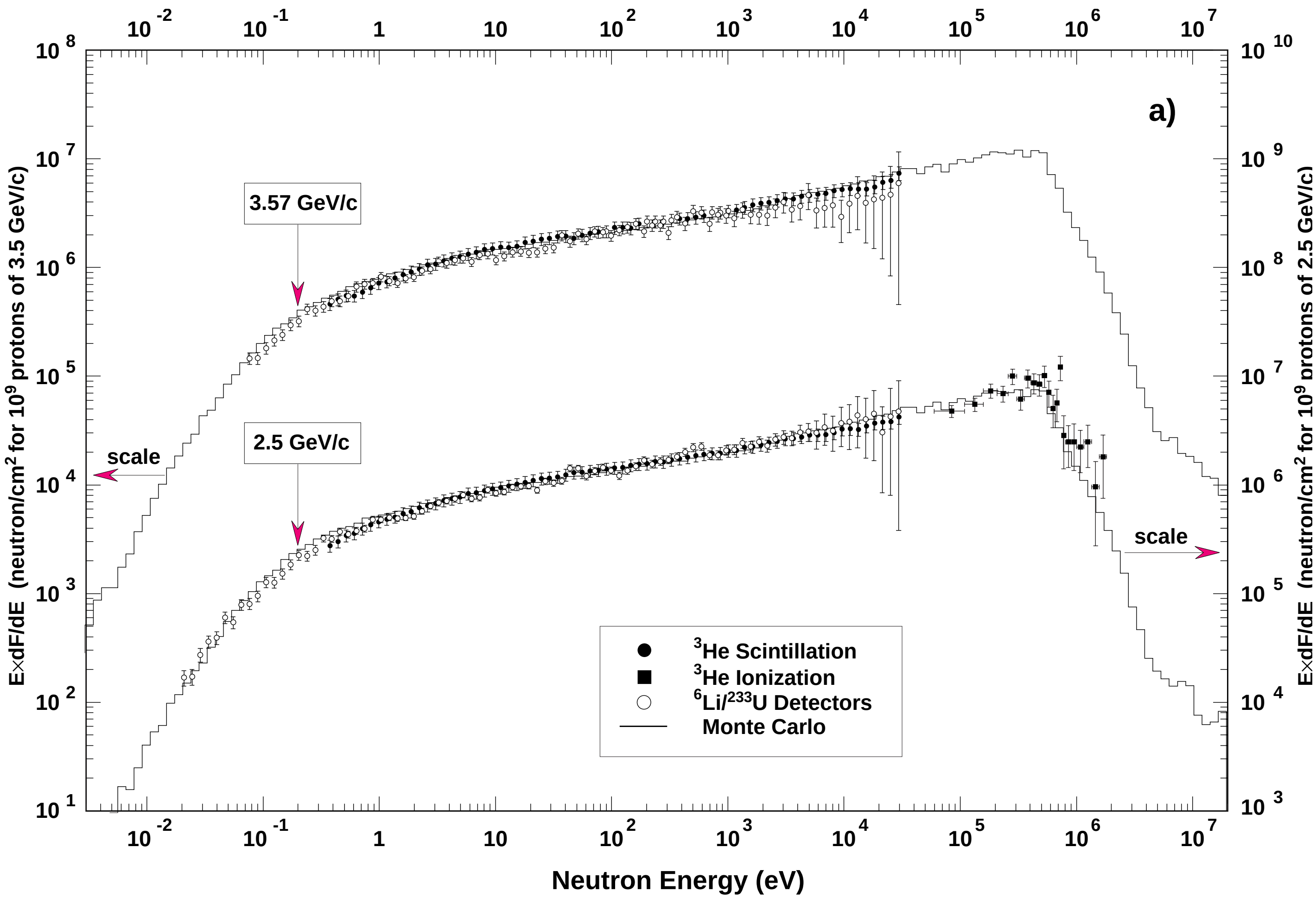

Neutron production examples: TARC (PLB458 167, NIMA478 577)

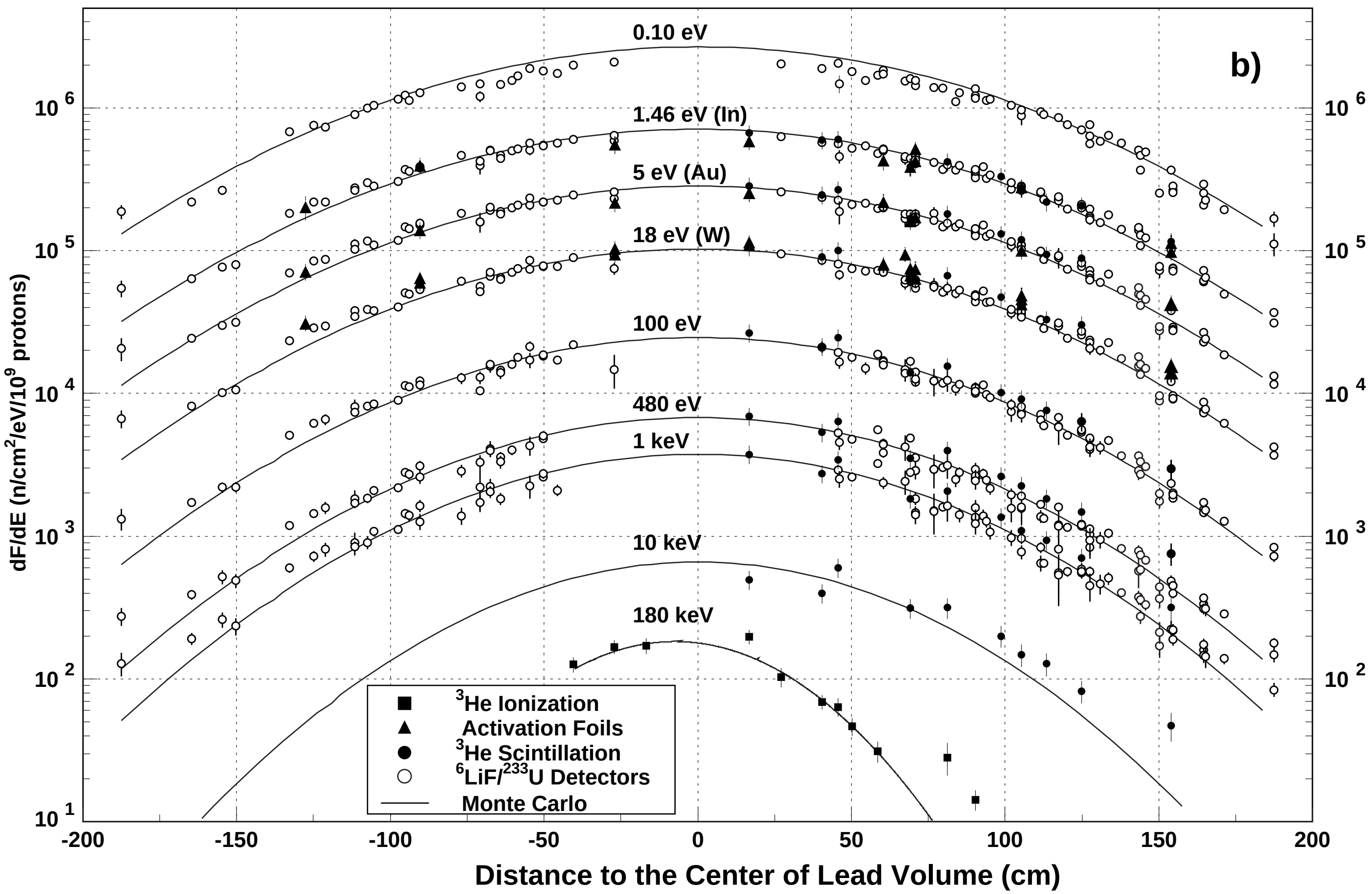

Motivations: Atmospheric neutrino fluxes (Astropart.Phys.**12** (2000) 315) (Milan)
Aircraft doses (Frascati, Siegen and GSF)

$\longrightarrow$ Exploiting the reliability of FLUKA Hadronic interaction models

Results

- The first 3Dimensional MC simulation of ν production due to atmospheric showers
- Extensive benchmarking with muon and hadron data in atmosphere
- Photomuon production by cosmic rays
- Widespread applications to aircraft exposure evaluation

Past results obtained in the superposition model: primary nuclei are split into nucleons before interacting

Hadron/muon fluxes (Astropart. Phys. 17 (2002) 477), FLUKA and CAPRICE94 data

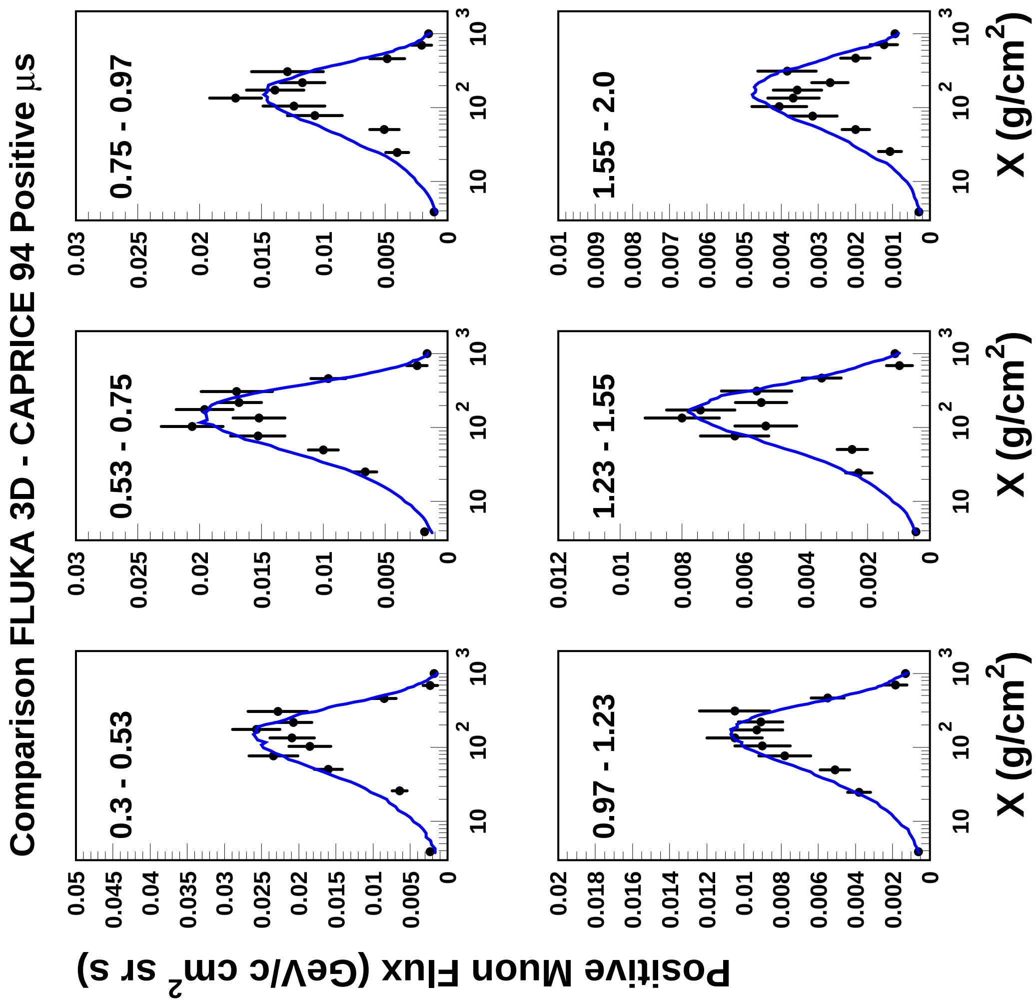

Hadron/muon fluxes in the atmosphere: examples

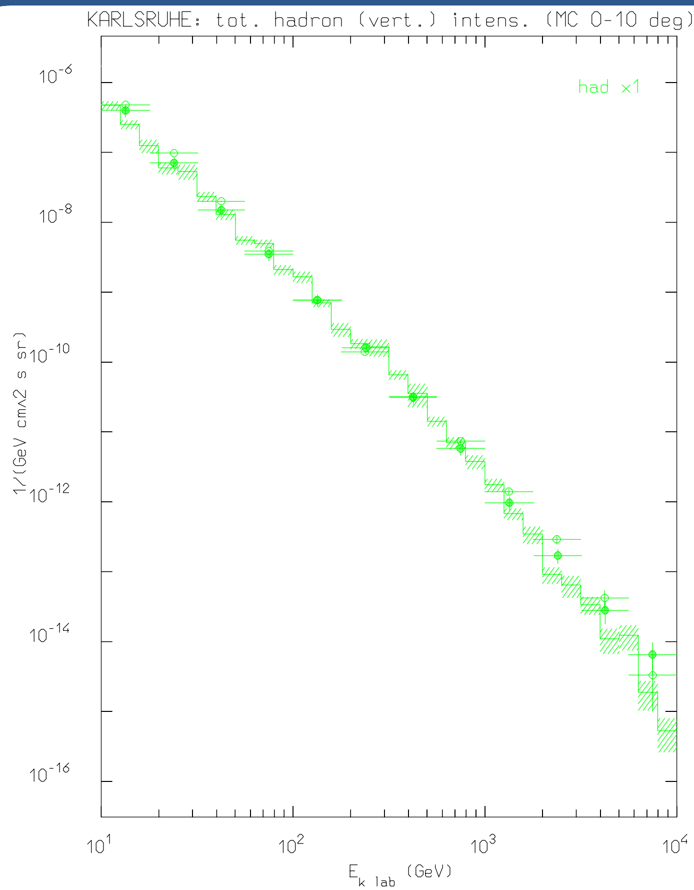

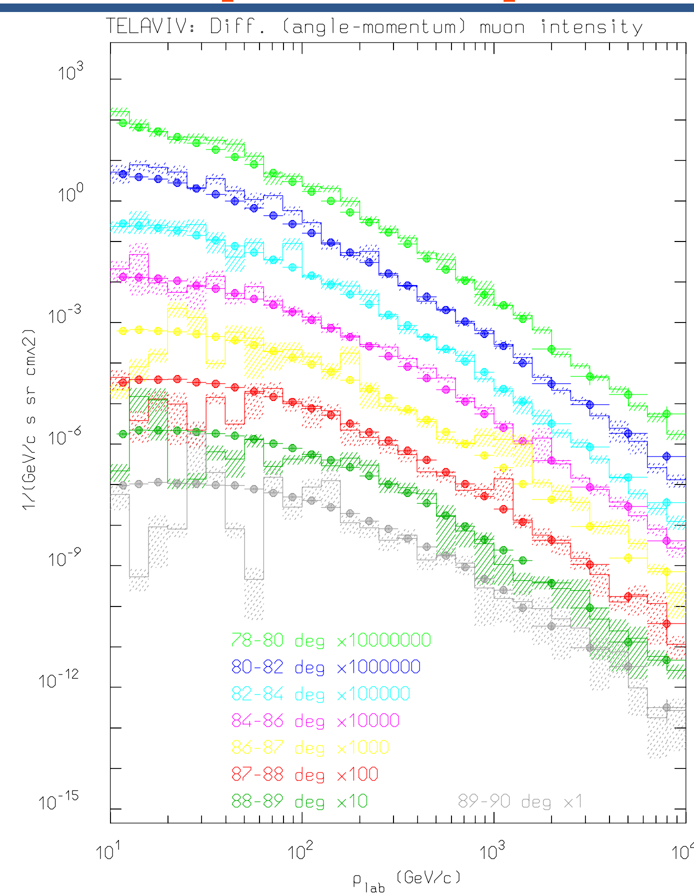

Hadron flux at sea level, KASKADE data from H. Kornmayer et al, JPG 21, 439 (1995).

Double differential muon fluxes in Tel Aviv. Data: O.C. Allkofer et al. NPB 259, 1, (1985).

Hadron/muon fluxes in the atmosphere: examples II
(Rad.Prot.Dosim.98 (2002) 367)

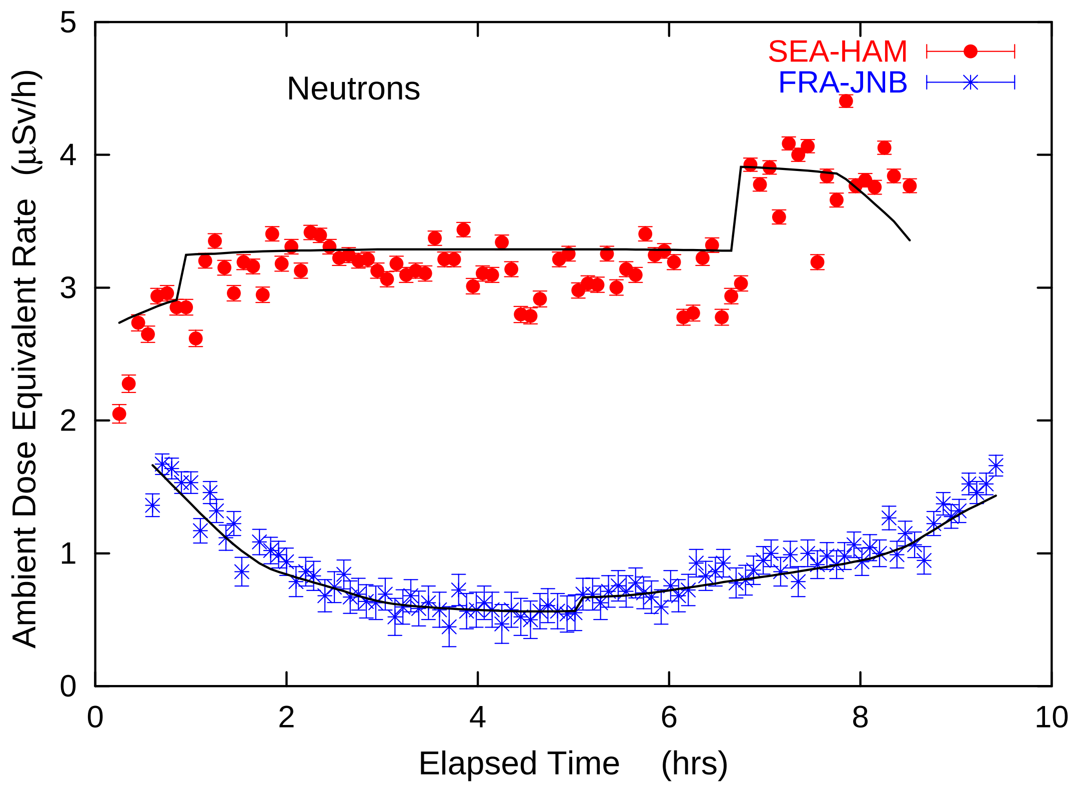

Ambient dose equivalent from neutrons measured during solar maximum on commercial flights from Seattle to Hamburg and from Frankfurt to Johannesburg, as function of time after take-off (symbols, exp. data, Lines: FLUKA).

Hadron/muon fluxes in the atmosphere: examples III (Rad.Prot.Dosim.98 (2002) 367)

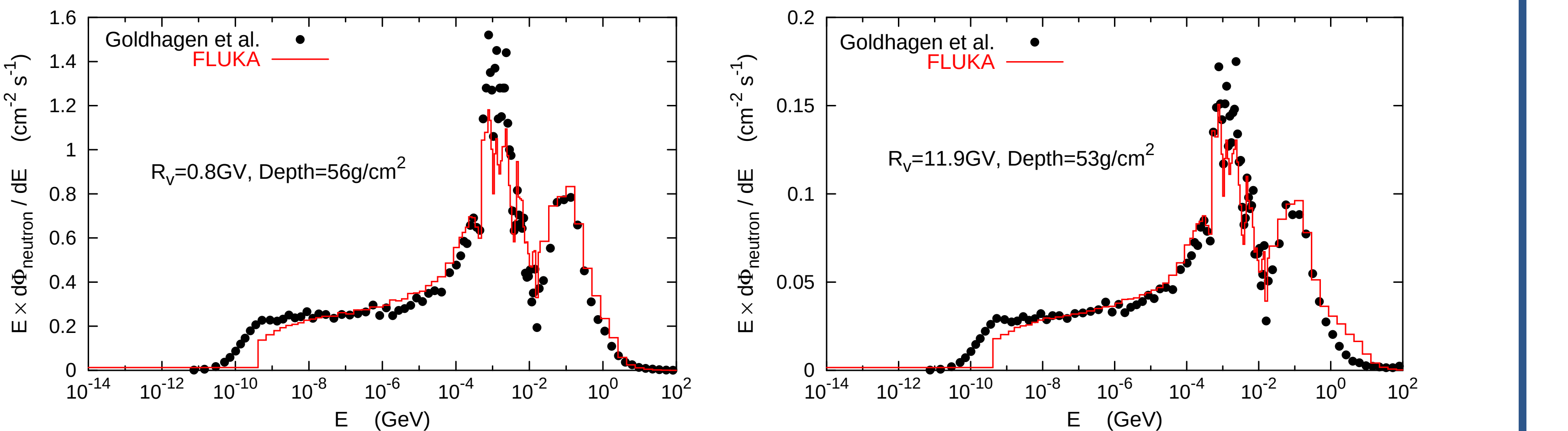

Atmospheric neutron spectra measured aboard of an ER-2 high-altitude airplane (NIM A476, 42 (2002)) (symbols) and calculated with FLUKA (histograms), at two different geographic locations and altitudes.